





Article

Daily Estimates of Global Radiation in the Brazilian Amazon from Simplified Models

Charles Campoe Martim ¹, Rhavel Salviano Dias Paulista ^{1,2} , Daniela Castagna ^{1,2}, Daniela Roberta Borella ² , Frederico Terra de Almeida ^{2,3} , João Gabriel Ribeiro Damian ⁴ and Adilson Pacheco de Souza ^{1,2,3,*} 

¹ Postgraduate Program in Environmental Physics, Federal University of Mato Grosso, Cuiaba 78060-900, MT, Brazil; charles.martim@sou.ufmt.br (C.C.M.); rhavel.paulista@sou.ufmt.br (R.S.D.P.); daniela.castagna@sou.ufmt.br (D.C.)

² Postgraduate Program in Environmental Sciences, Federal University of Mato Grosso, Sinop 78550-728, MT, Brazil; daniela.borella@sou.ufmt.br (D.R.B.); frederico.almeida@ufmt.br (F.T.d.A.)

³ Institute of Agrarian and Environmental Sciences, Federal University of Mato Grosso, Sinop 78550-728, MT, Brazil

⁴ Faculty of Exact and Technological Sciences, Mato Grosso State University, Sinop 78550-000, MT, Brazil; joao.gabriel.ribeiro@unemat.br

* Correspondence: adilson.souza@ufmt.br; Tel.: +55-66981363805

Abstract: Solar radiation is an element and a meteorological factor that is present in several processes, such as evapotranspiration, photosynthesis, and energy generation, among others. However, in some regions, there is a limitation in surface data measurements. In this study, 87 empirical models were evaluated to estimate global radiation (Hg) in the Brazilian Amazon biome; these models were divided into five groups according to the input variables, such as insolation (group I), air temperature (group II), relative humidity (group III), astronomical variables (group IV), and hybrid models (group V). The estimates were evaluated by their significance (*t*-test) and then according to the statistical metrics of the models' performance (R^2 , MBE, RMSE, and *d*). The group V model $[Hg/H_0 = a + b\ln\Delta T + c(S/S_0)^d]$ presented the best statistical performance in all the evaluated indicators, followed by the group I model $[Hg/H_0 = a + b(S/S_0)^c]$, and then the group II model $[Hg/H_0 = a + b\Delta T + c\Delta T^{0.25} + d\Delta T^{0.5} + e(T_{med}/H_0)]$. The group III models presented a low statistical performance, and the group IV models were not significant (NS) in all the evaluated meteorological stations. In general, it was found that the simplified or hybrid models based on insolation and air temperature were efficient in estimating Hg in the Brazilian Amazon biome.

Keywords: solar radiation; solar energy; minimum meteorological data; empirical estimation models; statistical indicators; Amazon biome



Citation: Martim, C.C.; Paulista, R.S.D.; Castagna, D.; Borella, D.R.; de Almeida, F.T.; Damian, J.G.R.; de Souza, A.P. Daily Estimates of Global Radiation in the Brazilian Amazon from Simplified Models. *Atmosphere* **2024**, *15*, 1397. <https://doi.org/10.3390/atmos15111397>

Academic Editors: Yanbo Shen and Abhnil Prasad

Received: 4 October 2024

Revised: 11 November 2024

Accepted: 16 November 2024

Published: 20 November 2024



Copyright: © 2024 by the authors. Licensee MDPI, Basel, Switzerland. This article is an open access article distributed under the terms and conditions of the Creative Commons Attribution (CC BY) license (<https://creativecommons.org/licenses/by/4.0/>).

1. Introduction

Solar radiation is a clean, abundant, continuous, and renewable energy source with great potential for expanding its use in Brazil and worldwide. In the current context, the spatial and temporal variability of the incidence of global radiation (Hg) on the Earth's surface can be considered one of the main drivers of its use, especially in climate change [1–3]. These variations, according to Souza et al. [4], depend on the Earth's movements (rotation and translation), geographic factors (latitude, longitude, altitude, orientation, and inclination of the surface), and atmospheric factors, such as clouds and interactions with greenhouse gases, aerosols, and water vapor [5–7]. All these factors generate great uncertainties in obtaining solar radiation, especially for short temporal partitions such as instantaneous, hourly, or daily values [8].

In short, when passing through the atmosphere, the electromagnetic waves that form solar radiation can be attenuated by reflection, absorption, and diffusion due to contact with the gases that make up the atmosphere, clouds, and/or suspended particles. However,

these phenomena are insufficient to retain the entire spectrum of electromagnetic waves from solar radiation. A percentage passes through the atmosphere without any interaction (direct radiation), which, together with the diffuse component (selective and non-selective, depending on the dimensions of the attenuating particle), hits the ground surface, forming global radiation—Hg [4].

Knowledge of global radiation incidence on natural and/or forced surfaces with different inclination angles and exposure faces can be applied in many scientific and technological areas. Accurate information on Hg is widely needed in several chemical, physical, and biological applications and processes [9] and in several sectors, such as renewable energy, meteorology, agriculture, hydrology, ecology, environmental comfort, epidemiology, and industry [10,11].

Despite its importance, in many regions, especially in underdeveloped countries, measuring Hg is still a challenge due to the high costs of instruments (sensors) and their periodic recalibration and maintenance needs; these activities are recurrent and necessary in meteorological stations, even if they are automatic [12]. In addition, Hg datasets are often characterized by many measurement failures or inconsistent data, mainly due to lack of maintenance (dirt deposited on sensors, shading, and a lack of sensor calibration). These problems occur even in countries with a high density of Hg monitoring stations [5,13,14]. Therefore, great efforts have been made to estimate Hg based on meteorological variables with lower monitoring costs that are widely available and monitored at meteorological stations worldwide [1].

In Brazil, this reality is no different, especially in the Amazon biome, which is located in the north of the country and occupies 49% of the national territory; this region has the lowest ratio between automatic meteorological stations (AMSs) and conventional meteorological stations (CMCs) per area of the station network of the National Institute of Meteorology (INMET). In addition to the low number of stations installed for surface monitoring, the percentages of failures in the existing databases vary from 10 to 60% [15–17], thus limiting seasonal assessments of the behavior of Hg incidence. Even in countries that invest more in research, these problems are observed, as reported by Fan et al. [10], evaluating 122 meteorological stations in China, who observed failures of 0.3 to 7.5% in the databases.

The spatial-temporal characterization of global radiation requires a series of long-term measurements. Despite the importance and interest of the scientific and governmental community, knowledge of this is still developing in the Amazon biome. This is mainly due to the large territorial extension, limited land access, and low population density (in terms of number of cities). Information on daily Hg levels in this biome is necessary for several applications associated with environmental sciences, since solid scientific evidence indicates that a representative part of this ecosystem is being affected by anthropogenic actions, particularly by the expansion of agricultural activities, the increasing frequency and severity of forest fires, and the degradation of and reduction in natural vegetation [18–20].

To meet the relevant needs for obtaining global radiation data, several models have been developed for Hg estimates based on other meteorological data and have been commonly made available/evaluated worldwide [16,21,22]. It is no different for regions such as the Brazilian Amazon, where, despite some studies having already been carried out [15,17], there is still a need to evaluate simplified Hg estimation models for constructing continuous data series for agricultural and environmental applications.

Evaluations of simplified and/or parameterized models for Hg estimates require regional calibrations of the statistical coefficients that can provide good estimates through indirect relationships with other meteorological variables, as long as these are simple to monitor, have greater database availability, or have a good correlation with Hg, as is the case with insolation, air temperature, relative humidity, and rainfall [9–12,23].

The first empirical model for estimating Hg based on insolation (S) was proposed by Angström [24] and later modified by Prescott [25]; in honor of the authors, it became known as the Angstrom–Prescott (A-P) model. Regarding air temperature, the first simplified model was proposed by Hargreaves and Samani [26], when they proved that the daily

thermal amplitude ($\Delta T = T_{\max} - T_{\min}$) presents good correlations with Hg incidence; later, Bristow and Campbell [27] proved that there is an exponential correlation between ΔT and Hg.

Studies based on insolation present a superior performance when compared to studies based on other meteorological variables, such as air temperature [28,29]; however, in the Brazilian context, the availability of insolation data is lower for most biomes and states, unlike air temperature, which is measured in practically all CMSs and AMSs [30,31]; this disparity is more pronounced in the context of the Brazilian Amazon. Therefore, there are several possibilities for adjusting the models based on other meteorological or geographic variables that correlate with Hg, as this allows for increased application possibilities for different situations according to data availability and improves Hg's predictive capacity.

After the widespread dissemination of the Angstrom–Prescott [25], Hargreaves and Samani [26], and Bristow and Campbell [27] models, several authors proposed modifications such as polynomial, logarithmic, potential, and exponential adjustments. In a literature review, Pietro and García (2022) [11] reported the existence of 165 different models, which can be classified according to the meteorological and non-meteorological variables used: (i) models based on insolation (S), in hours (group I); (ii) models based on maximum, average, and minimum air temperatures, in °C (group II); and (iii) models that consider combinations of variables, such as insolation; maximum, average and minimum air temperatures; relative humidity; latitude; atmospheric pressure; solar declination; wind speed; and rainfall (group III). Empirical models have been studied in different regions of the world for Hg estimates on a daily scale, especially based on these three groups mentioned above. Highlights include studies based on insolation (S) for China [9,22,32,33], Spain [34], Turkey [35–38], Sudan [39], Egypt [40], Saudi Arabia [41], Nigeria [29], Iran [21], and South Korea [42].

Therefore, other studies involving models based on air temperature (daily maximum, average, and minimum) were developed for different locations by different authors, such as Egypt [12], China [1,9,10,22,43–45], United States [23,27,46–48], Italy [23], United Kingdom [23], Netherlands [23], South Africa [23], Australia [23], Nigeria [28,29,49], Saudi Arabia [50], Africa [51], Iran [21,52], India [2,53], and Turkey [14]; models based on relative humidity were in Nigeria [28], Bahrain [54], Turkey [55], and Nigeria [29,49]; models based on astronomical variables in Jordan [56], Turkey [37,55], and Nigeria [29]; and hybrid models in China [9,10,22,32,45], Nigeria [28,29,49,57,58], Sudan [54], Bahrain [54], Saudi Arabia [41], Turkey [14,55], and South Korea [42].

The most comprehensive study involving Hg estimates was conducted in the Amazon biome with the Angstrom–Prescott model for 20 meteorological stations (MSs) [17]; however, this article was based on only two Hg estimation models. Studies developed in several regions of Brazil also presented point estimates for some locations in the Amazon [4,15,16,59]. In all cases, the importance of understanding the dynamics of the region's atmosphere was highlighted in the estimates. One of the simplest ways to understand the behavior of the atmosphere based on solar radiation is through atmospheric transmissivity indices or a clarity index (Kt), which shows the ratio between global radiation (Hg) and extraterrestrial radiation (H_0). Several studies have been carried out to explore various models in different locations around the world, and many comparisons have been made to optimize and find the best models for estimating Hg as a function of the levels or classes of the clarity indices [60–62].

Given the environmental importance of this biome and Hg for several agro-environmental applications, the objective of this study was to evaluate and determine which models based on meteorological and astronomical variables present the best performance in estimating daily global radiation (Hg) in the Brazilian Amazon, using meteorological and astronomical variables.

2. Materials and Methods

2.1. Study Area

The study area is concentrated in the Brazilian Amazon biome, which encompasses a large area of 4,196,943 km² distributed across nine states: Acre, Amapá, Amazonas, Pará, Rondônia, Roraima, part of Tocantins, Mato Grosso, and Maranhão (Figure 1). Twenty locations with meteorological stations (MSs) that presented simultaneous automatic (MSAs) and conventional (MSCs) measurements (Table 1) were selected, considering the following daily databases: (i) MSAs—maximum, average, and minimum temperature (T_{max}, T_{med}, and T_{min}); average relative humidity (RH_{med}); and global horizontal radiation (Hg); (ii) MSCs—insolation (S). These databases were obtained from the website of the National Institute of Meteorology (INMET) (<https://portal.inmet.gov.br/> accessed on 3 March 2023). Although the INMET station network is larger than that selected in this study for the Amazon region, it is worth noting that only those that presented concomitant measurements of Hg and S were selected.

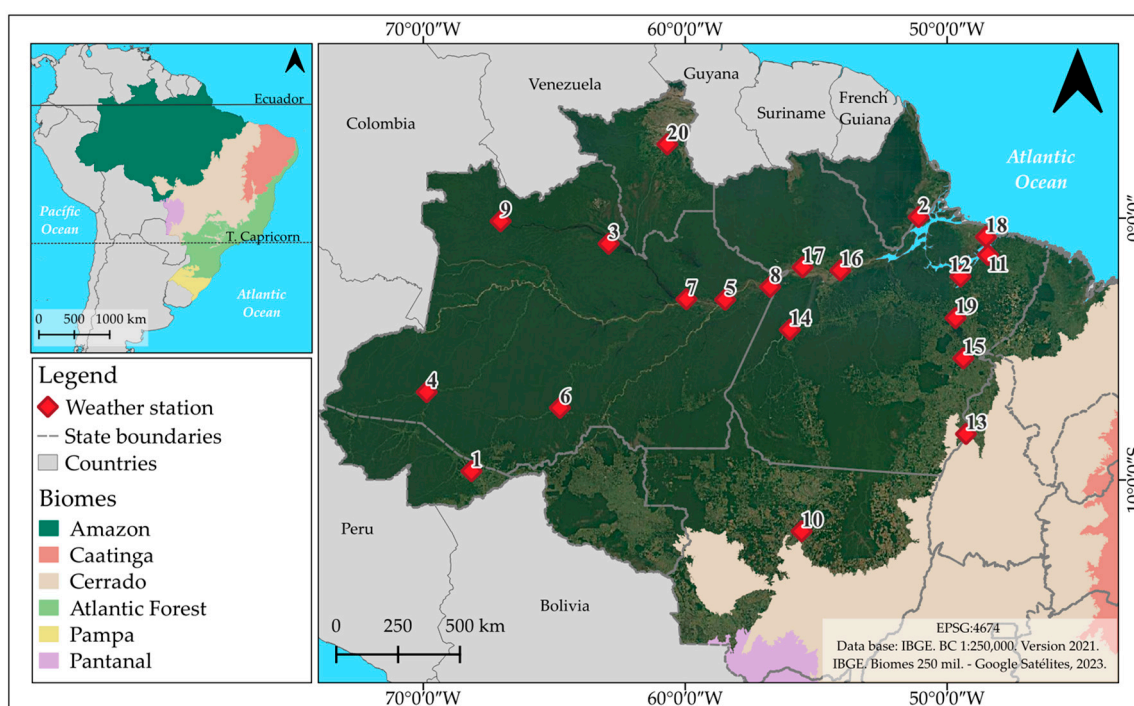


Figure 1. The location of the 20 meteorological stations evaluated in this study in the Amazon biome, Brazil (the numerical order of the stations—“1–20”—is presented in Table 1) [63,64].

According to the Köppen classification (KCC), the 20 stations included three subclasses of tropical climates—Am (monsoon), Af (with a dry season), and Aw (with a dry winter)—with high precipitation (over 3600 mm year⁻¹) in the north of the biome and with a reduction towards the south of the Amazon [65]. Geographically, the AMSs and CMSs were located between latitudes 0.035° to −11.97° and longitudes −48.43° to −69.87° (in three distinct time zones), while altitudes varied from 9 to 366 m. The longest data series evaluated was twenty-two years (2000 to 2022) at the Manaus station (AM), and the shortest data series was five years (2012 to 2017) at the Soure station (PA) (Table 1).

The meteorological data were subjected to filters to identify inconsistencies and failures [66], in which case days that presented daily failures of T_{max}, T_{med}, T_{min}, S, and RH_{med} and hourly failures of Hg between 10 am and 2 pm (local solar time) were excluded; days with an insolation ratio (R_i) > 1.0 and K_t > 0.85 were also excluded. Subsequently, by AMS, the data series was divided into 70% for calibration of the model coefficients, and the remainder (30%) was used to evaluate the statistical performance. This separation of the

databases ensured the representativeness and proportionality of the periods of the year (months) in both databases.

Table 1. Meteorological stations in the Brazilian Amazon and their respective locations, climate classification, geographic coordinates, and data period.

State	Meteorological Station	KCC *	Lat. (°)	Lon. (°)	Alt. (m)	Data Period
Acre (AC)	1—Rio Branco	Am	−9.67	−68.16	163	2015–2022
Amapá (AP)	2—Macapá	Am	0.035	−51.08	16	2013–2022
Amazonas (AM)	3—Barcelos	Af	−0.98	−62.92	29	2008–2022
	4—Eirunepé	Af	−6.65	−69.87	121	2012–2022
	5—Itacoatiara	Af	−3.12	−58.47	41	2008–2022
	6—Lábrea	Am	−7.25	−64.78	61	2008–2018
	7—Manaus	Af	−3.1	−59.95	61	2000–2022
	8—Parintins	Af	−2.63	−56.75	18	2008–2018
	9—São Gabriel da Cachoeira	Af	−0.12	−67.05	79	2011–2022
Mato Grosso (MT)	10—Sinop	Aw	−11.85	−55.55	366	2006–2017
Pará (PA)	11—Belém	Af	−1.41	−48.43	21	2003–2022
	12—Cametá	Af	−2.23	−49.48	9	2008–2022
	13—Conceição do Araguaia	Aw	−8.25	−49.27	175	2008–2022
	14—Itaituba	Af	−4.27	−56.00	24	2008–2022
	15—Marabá	Aw	−5.36	−49.37	116	2009–2022
	16—Monte Alegre	Am	−2	−54.07	100	2012–2022
	17—Óbidos	Am	−1.88	−55.51	89	2012–2017
	18—Soure	Am	−0.72	−48.51	12	2008–2017
	19—Tucuruí	Am	−3.82	−49.67	137	2008–2017
Roraima (RR)	20—Boa Vista	Am	2.82	−60.68	82	2010–2022

Latitude (Lat.); longitude (Lon.); and altitude (Alt.). * KCC are Koppen climate classes according to * Alvares et al. [60].

2.2. Simplified Models for Estimating Global Radiation (H_g)

All simplified models evaluated are based on extraterrestrial radiation (H_0), which corresponds to radiation that has not yet interacted with atmospheric elements; this variable was obtained by Equation (1), which depends on the eccentricity factor of the Earth’s orbit (dr —Equation (2)), solar declination (δ —Equation (3)), and the daily hour angle (h —Equation (4)). In addition to H_0 , some simplified models depend on the photoperiod (S_0 —Equation (5)), atmospheric transmissivity (K_t —which represents the fraction of radiation that reaches the Earth’s surface—Equation (6)), or the insolation ratio (R_i —which represents the fraction of time of the incidence of direct radiation throughout a day—Equation (7)) [15,67].

$$H_0 = 37.59 \times dr \times \left(\frac{\pi}{180} \times h \times \text{sen}\phi \times \text{sen}\delta + \cos\phi \times \cos\delta \times \text{sen}h \right) \tag{1}$$

$$dr = 1 + 0.033 \times \cos\left(\frac{360 \times DJ}{365}\right) \tag{2}$$

$$\delta = 23.45 \times \text{sen}\left[\frac{360}{365}(DJ + 284)\right] \tag{3}$$

$$h = \cos^{-1}(-\tan\phi \times \tan\delta) \tag{4}$$

$$S_0 = \frac{2 \times h}{15} \tag{5}$$

$$K_t = \frac{H_g}{H_0} \tag{6}$$

$$Ri = \frac{S}{S_0} \tag{7}$$

where ϕ is the local latitude of the stations ($^\circ$); δ and dr are dependent only on the time of year (DJ), which indicates the ordering of the days throughout the year ($1 \leq DJ \leq 365$ or 366 days); h is dependent on the time of year and latitude; and the values of K_t and R_i are dimensionless.

Based on the literature review, 87 simplified models for daily Hg estimates were obtained, presenting differences in the input variables or the analytical estimation model. These models were divided into 5 groups according to the input variables, generating the following combinations:

- Group I: empirical models based on insolation (S), photoperiod (S_0), and extraterrestrial radiation (H_0) (Table 2);
- Group II: empirical models based on maximum, mean, and minimum air temperature (T_{max} , T_{med} , and T_{min}) and extraterrestrial radiation (H_0) (Table 3);
- Group III: empirical models based on relative humidity (RH) and extraterrestrial radiation (H_0) (Table 4);
- Group IV: empirical models with astronomical variables, such as solar declination (δ), Julian day (DJ), and extraterrestrial radiation (H_0) (Table 4);
- Group V: hybrid empirical models, based on two or more variables such as S, T_{max} , T_{med} , T_{min} , RHmed, latitude (ϕ), photoperiod (S_0), and extraterrestrial radiation (H_0) (Table 5).

Table 2. Empirical models for indirect estimates of global radiation, based on insolation.

N°	References	Models
1	Angström [24]; Prescott [25]	$Hg/H_0 = a + b(S/S_0)$
2	Ögelman et al. [36]	$Hg/H_0 = a + b(S/S_0) + c(S/S_0)^2$
3	Bahel [68]	$Hg/H_0 = a + b(S/S_0) + c(S/S_0)^2 + d(S/S_0)^3$
4	Newland [33]	$Hg/H_0 = a + b(S/S_0) + c \ln(f(S)/S_0)$
5	Togrul and Onat [37]	$Hg/H_0 = a + b/H_0 + c(S/S_0)/H_0$
6	Togrul et al. [38]	$Hg/H_0 = a + b \ln(f(S)/S_0)$
7	Almorox and Hontoria [34]	$Hg/H_0 = a + b \text{EXP}(S/S_0)$
8		$Hg/H_0 = a \text{EXP}(bS/S_0)$
9	Elagib and Mansell [39]	$Hg/H_0 = a(S/S_0)^b$
10		$Hg/H_0 = a + b(S/S_0)^c$
11	El-Metwally [40]	$Hg/H_0 = a^{1/(f(S)/S_0)}$
12	Bakirci [35]	$Hg/H_0 = a + b \text{EXP}(S/S_0) + c(S/S_0)$
13	Li et al. [43]	$Hg/H_0 = a + b/H_0 + c S/H_0$

Table 3. Empirical models of daily estimates of global radiation based on air temperature.

N°	References	Models
14	Hargreaves and Samani [26]	$Hg/H_0 = a\Delta T^{0.5}$
15	Bristow and Campbell [27]	$Hg/H_0 = a(1 - \text{EXP}(-b\Delta T^c))$
16	Hargreaves et al. [51]	$Hg/H_0 = a + b\Delta T^{0.5}$
17	Ertekin and Yaldiz [55]	$Hg/H_0 = a + b/H_0 + c * (T_{med}/H_0)$
18	Goodin et al. [46]	$Hg/H_0 = a * (1 - \text{EXP}(-b * \Delta T^c/H_0))$
19	Thornton and Running [47]	$Hg/H_0 = 1 - \text{EXP}(-a * \Delta T^b)$
20	Weiss et al. [48]	$Hg/H_0 = 0.75 * (1 - \text{EXP}(-a * \Delta T^2/H_0))$
21	Chen et al. [22]	$Hg/H_0 = a + b * \ln \Delta T$
22	Abraha and Savage [23]	$Hg/H_0 = 0.75 * (1 - \text{EXP}(-a * \Delta T^2/\Delta T_{med}))$

Table 3. Cont.

N°	References	Models
23	Falayi et al. [29]	$Hg/H_0 = a + b * Tmin$
24		$Hg/H_0 = a + b * Tmax$
25	Panday and Katiyar [53]	$Hg/H_0 = a + b * Tmax/Tmin$
26		$Hg/H_0 = a + b * Tmax/Tmin + c * (Tmax/Tmin)^2$
27		$Hg/H_0 = a + b * Tmax/Tmin + c * (Tmax/Tmin)^2 + d * (Tmax/Tmin)^3$
28	Adaramola [28]	$Hg/H_0 = a + b * Tmed$
29		$Hg/H_0 = a + b * Tmin/Tmax$
30	Chen and Li [9]	$Hg/H_0 = a + b * \Delta T$
31		$Hg/H_0 = a + b * Tmin + c * Tmax + d * Tmin * Tmax$
32		$Hg/H_0 = a + b * Tmin + c * Tmax$
33	Li et al. [32]	$Hg/H_0 = a/H_0 + b * Tmin + c * Tmax$
34	Benghanem and Mellit [50]	$Hg/H_0 = a/H_0 + b * \Delta T^c$
35	Li et al. [44]	$Hg/H_0 = a + (b + c * Tmed) * \Delta T^{0.5}$
36	Hassan et al. [12]	$Hg/H_0 = a + b * \Delta T^c$
37		$Hg/H_0 = a + b * H_0 * Tmed^c$
38		$Hg/H_0 = a * H_0 * Tmed^b$
39		$Hg/H_0 = a * EXP(b * Tmed^c)$
40		$Hg/H_0 = a + b * Tmed + c * Tmed^2$
41		$Hg/H_0 = (a + b * \Delta T + c * \Delta T^2) * \Delta T^d$
42	Jahani et al. [21]	$Hg/H_0 = a + b * \Delta T + c * \Delta T^2 + d * \Delta T^3$
43		$Hg/H_0 = a + b * \Delta T^{0.5} + c * \Delta T^{1.5} + d * \Delta T^{2.5}$
44	Fan et al. [10]	$Hg/H_0 = a + b * \Delta T + c * \Delta T^{0.25} + d * \Delta T^{0.5}$
45		$Hg/H_0 = a + b * \Delta T + c * \Delta T^{0.25} + d * \Delta T^{0.5} + e * Tmed/H_0$

Table 4. Empirical models of daily estimates of global radiation based on relative air humidity (RHmed) and astronomical variables (δ , H_0 , and DJ).

N°	References	Models
46	Elagib et al. [39]	$Hg/H_0 = a/H_0 + b * RHmed/H_0$
47		$Hg/H_0 = a/H_0 + b * (RHmed - H_0)/H_0$
48	Falayi et al. [29]	$Hg/H_0 = a + b * RHmed$
49	Kolebaje et al. [49]	$Hg/H_0 = a + b * RHmed^{0.5}$
50	Ertekin and Yaldiz [55]	$Hg/H_0 = a/H_0 + b * \delta/H_0$
51	Togrul and Onat [37]	$Hg/H_0 = a/H_0 + b * \text{sen}\delta/H_0$
52	Togrul and Onat [37]	$Hg/H_0 = a + b/H_0$
53	Al-Salaymeh [56]	$Hg/H_0 = a/H_0 + b * \text{sen}(2 * \pi * DJ/c + d)/H_0$
54	Al-Salaymeh [56]	$Hg/H_0 = (a + b * DJ + c * DJ^2 + d * DJ^3 + e * DJ^4)/H_0$

Table 5. Hybrid empirical models of daily estimates of global radiation with meteorological and astronomical variables.

N°	References	Models
55	Glover and McCulloch [69]	$Hg/H_0 = a * \cos\phi + b * (S/S_0)$
56	Swartman and Ogunlade [58]	$Hg/H_0 = a * EXP(b * (S/S_0 - RHmed))$
57		$Hg/H_0 = a + b * RHmed + c * S/S_0$
58		$Hg/H_0 = a * RHmed^b * (S/S_0)^c$
59	Ododo et al. [57]	$Hg/H_0 = a * Tmed^b * Tmed^c * (S/S_0)^d$
60		$Hg/H_0 = a + b * Tmed + c * RHmed + d * Tmed + e * (S/S_0)$

Table 5. Cont.

N°	References	Models
61	Elagib et al. [39]	$Hg/H_0 = a/H_0 + b * (RHmed - \Delta T - H_0)/H_0$
62	Chen et al. [22]	$Hg/H_0 = a + b * \ln\Delta T + c * (S/S_0)^d$
63	Falayi et al. [29]	$Hg/H_0 = a + b * Tmed + c * (S/S_0)$
64		$Hg/H_0 = a + b * Tmin + c * (S/S_0)$
65		$Hg/H_0 = a + b * Tmax + c * (S/S_0)$
66		$Hg/H_0 = a + b * Tmed + c * RHmed + d * (S/S_0)$
67	El-Sebaili et al. [41]	$Hg/H_0 = a + b * Tmed + c * RHmed$
68	Adaramola [28]	$Hg/H_0 = a + b * (Tmin/Tmax) * RHmed/100$
69	Korachagaon and Bapat [70]	$Hg/H_0 = a + b * Tmax + c * \Delta T + d * RHmed$
70		$Hg/H_0 = a + b * Tmax + c * Tmin + d * \Delta T + e * RHmed$
71	Chen and Li [9]	$Hg/H_0 = a + b * \Delta T^{0.5} + c * (S/S_0)$
72		$Hg/H_0 = a + b * Tmin + c * Tmax + d * (S/S_0)$
73		$Hg/H_0 = a + b * Tmax + c * Tmin + d * RHmed + e * (S/S_0) RHmed + e (S/So)$
74		$Hg/H_0 = a + b * \Delta T^{0.5} + c * RHmed$
75	Li et al. [32]	$Hg/H_0 = a/H_0 + b * Tmin + c * Tmax + d * RHmed$
76		$Hg/H_0 = a/H_0 + b * Tmin + c * Tmax + d * RHmed/H_0$
77		$Hg/H_0 = a/H_0 + b * \sqrt{(\Delta T)} + c * RHmed$
78		$Hg/H_0 = a/H_0 + b * \sqrt{(\Delta T)} + c * (RHmed/H_0)$
79	Saffaripour et al. [52]	$Hg/H_0 = a + b/H_0 + c * Tmax/H_0 + d * (S/S_0)/H_0$
80		$Hg/H_0 = a + b/H_0 + c * RHmed/H_0 + d * (S/S_0)/H_0$
81		$Hg/H_0 = a + b * \sin\delta + c * (S/S_0)$
82	Lee [42]	$Hg/H_0 = a + b * (S/S_0)^c + d * \Delta T^e$
83	Li et al. [45]	$Hg/H_0 = a * (1 + b * RHmed) * \Delta T^{0.5}$
84		$Hg/H_0 = a * (1 + b * RHmed) * (1 - \text{EXP}(-c * \Delta T^d))$
85	Kolebaje et al. [49]	$Hg/H_0 = a + b * \Delta T/f(S)$
86		$Hg/H_0 = a + b * ((\Delta T + RHmed)/S_0)^{0.5}$
87	Yildirim et al. [14]	$Hg/H_0 = a + b * RHmed + c * S/S_0 + d * (S/S_0)^2 + e(S/S_0)^3$

Local calibrations of the estimates of the empirical coefficients (“a”, “b”, “c”, and “d”) of the simplified models were performed for each station with data grouping, using the iterative Gauss–Newton algorithm for nonlinear optimizations by the least squares method, in the Statistica 14.0.0.15 software (TIBCO Software Inc., Santa Clara, CA, USA), together with an evaluation of the maximization of the coefficient of determination (R²) and restrictions for Hg < H₀. Sequentially, the analyses for the groupings of the models are presented.

2.2.1. Simplified Models Based on Insolation (S)—Group I

The Angstrom–Prescott model was the precursor of this type of estimation (Table 2), which linearly correlates the insolation ratio (Ri) and atmospheric transmissivity (Kt); in this case, the linear coefficient (“a”) and angular coefficient (“b”) are dependent on regional atmospheric conditions and need to be calibrated locally. Although these coefficients are empirical, they describe two physical possibilities of Hg incidence: (i) when Ri tends to zero, the linear coefficient (a) indicates the minimum transmissivity of the atmosphere in the region, given by diffuse radiation; and (ii) when Ri tends to 1.0, the sum of the two coefficients indicates the maximum transmissivity of the atmosphere in the region on clear days and the contributions of diffuse and direct radiation [34].

This methodology is based on obtaining S using Campbell–Stockes heliographs (Hidromec, Rio de Janeiro, RJ, Brazil), positioned and aligned according to local latitude, showing the concentration and projection of solar rays in the heliograms, according to

the apparent diurnal movement of the Sun (the zenith angle). Although simplified, this analysis can indicate changes in the incidence pattern of direct radiation due to the increase in atmospheric multireflection and horizontal brightness when S tends to 0.0 [56]. Furthermore, it is worth noting that there may be an incidence of global radiation at a level below that necessary for the burning of heliograms (estimated at around 120 W m^{-2}); however, these energy levels can be computed as diffuse radiation in cloudy sky conditions [66].

Models 2 to 13 were developed as modifications to the Angstrom–Prescott model, with the insertion of second- and third-degree polynomial terms, logarithms, exponentials, and potentials, and are functions of the variables S , S_0 , and H_0 . It was necessary to insert the expression $f(S) = (S + 1)$ in place of S represented in models 4, 6, and 11 because these are models limited to days where there is no sunlight ($S = 0$). This condition represents 4.5% of the historical series of meteorological stations in the Amazon biome.

2.2.2. Simplified Models Based on Air Temperature (S)—Group II

In general, insolation (S) measurements are limited to a few meteorological stations [9,23]. For example, in China, “ S ” is monitored in only 30% of the country’s stations [1]; specifically, in the Amazon biome (the region of this study), it is around 27%. In developing countries, air temperature is typically the meteorological variable with the greatest spatial and temporal diffusion of measurements due to the sensors’ simplicity and wide application [51].

Models 14 to 45 (Table 3) are based on different daily correlations between H_g and statistical variations in air temperature, such as maximum temperature (T_{\max}), mean temperature (T_{med}), minimum temperature (T_{\min}), mean monthly thermal amplitude (ΔT_{med}), and daily thermal amplitude ($\Delta T = T_{\max} - T_{\min}$); these models can also be classified into five subgroups, depending on different combinations of the input variables: (T_{\max} , T_{\min} , H_0), (T_{med} , H_0), (T_{\min} , H_0), (T_{\max} , H_0), and (T_{\max} , T_{med} , T_{\min} , H_0).

2.2.3. Simplified Models Based on Relative Humidity or Astronomical Variables—Groups III and IV

In the literature, fewer models have been developed for these input variables since their relationships with global radiation are indirect, and they have longer response time intervals with H_g . Relative air humidity can be obtained by psychrometric sets (dry bulb and wet bulb) or capacitive sensors, and, in this case, in Brazilian conditions, there is greater availability of daily average values, with models 46 to 49 representing this group. In turn, models 46 to 54 are based on non-meteorological variables and are generally directly associated with the time of year, depending on solar declination (δ), the numerical ordering of the days throughout the year (DJ—Julian day), and extraterrestrial radiation (H_0) (Table 4).

2.2.4. Hybrid Models—Group V

Complex or hybrid models aim to improve the performance of the simplified empirical models [21], since, in addition to the direct influence of global radiation on air temperature or insolation, other astronomical and geographic factors can directly interfere with the incidence of radiation on the Earth’s surface [49]. Table 5 presents 33 models dependent on the relationships between ϕ , H_0 , S , S_0 , T_{\max} , T_{med} , T_{\min} , RH_{med} , ΔT , and δ .

2.3. Statistical Performance of Empirical Models

After local calibrations of the coefficients of each model, the t -test (which is a hypothesis test) was performed to assess the significance (with an adopted value of $p < 0.05$) of the model coefficient (β_a) concerning the standard error of the estimated coefficient (SE_{β_a}) to verify the possibility of using the coefficients and models in the estimation of H_g (Equation (8)).

$$\text{Test} - t = \frac{\beta_a}{SE_{\beta_a}} \quad (8)$$

In the literature, several statistical indicators evaluate the performance of the statistical or parametric models used in meteorological and climate estimates, including for obtaining Hg [71,72]. In general, the use of the root mean square error (RMSE), mean bias error (MBE), Willmott's "d" index, and the coefficient of determination or R^2 (Equations (9)–(12), respectively) has been recommended.

According to Adaramola [28], the MBE indicator, when positive, represents overestimates, and, when negative, indicates underestimates of the variable studied; the disadvantage of this indicator is that high values with different signs may end up canceling each other out, generating a small error, which impairs the analysis of the estimation model. The RMSE index, on the other hand, is represented only by positive values, with values close to zero being ideal. Since it is a quadratic function, large variations in the data can increase the values; that is, it is a metric of how the estimated values are spread around the measured ones. The Willmott index or "d" is an indicator that provides dimensionless values between 0 and 1, and the higher the value, the better the model's performance. The coefficient of determination or R^2 indicates the quality of the linear relationship between the measured values (the independent variable) and estimated values (the dependent variable), which varies from 0 to 1, with values closer to 1 indicating better estimates. Although there are several statistical indicators, it is not recommended to use only one quality of fit index in isolation; that is, several indicators should be used together, as they may present different or similar responses regarding the statistical performance of the models analyzed [10,72].

$$\text{RMSE} = \left[\frac{\sum_{i=1}^N (P_i - O_i)^2}{N} \right]^{\frac{1}{2}} \quad (9)$$

$$\text{MBE} = \left[\frac{\sum_{i=1}^N (P_i - O_i)}{N} \right] \quad (10)$$

$$d = 1 - \left[\frac{\sum_{i=1}^N (P_i - O_i)^2}{\sum_{i=1}^N (|P_i - O| + |O_i - O|)^2} \right] \quad (11)$$

$$R^2 = 1 - \frac{\sum_{i=1}^n (P_i - O_i)^2}{\sum_{i=1}^n (O_i - O)^2} \quad (12)$$

where P_i is the estimated value; O_i is the reference value observed at the meteorological stations; O is the average of the reference values; and N is the number of observations.

3. Results

Although the Brazilian Amazon biome has a tropical climate, variability was observed between the averages of the meteorological variables in the different seasons evaluated (Table 6). The annual averages and standard errors of the Hg averages ranged from 15.1 ± 3.59 (Belém) to 20.6 ± 4.19 $\text{MJ m}^{-2} \text{d}^{-1}$ (Monte Alegre) and generated average atmospheric transmissivity coefficients of 0.42 ± 0.12 (Belém) to 0.57 ± 0.11 (Monte Alegre); the annual averages of sunshine (S) ranged from 3.94 ± 2.70 (Eirunepé) to 7.57 ± 2.59 h (Cameté), totaling sunshine ratios of 0.33 ± 0.22 (Eirunepé) to 0.63 ± 0.21 (Monte Alegre). Regarding air temperatures, variations of 30.94 ± 0.95 °C (Soure) to 33.54 ± 2.75 °C (Conceição do Araguaia) were observed for T_{max} ; from 25.41 ± 1.63 °C (Sinop) to 27.83 ± 1.56 °C (Roraima) for T_{med} ; and from 20.16 ± 2.11 °C (Sinop) to 25.34 ± 1.51 °C (Soure) for T_{min} ; therefore, the annual RH_{med} varied from 68.54 ± 10.17 (Roraima) to $83.88 \pm 6.11\%$ (Barcelos), and the total annual rainfall ranged from 1616 ± 100 (Roraima) to 3205 ± 129 mm (Belém). The annual averages of the theoretical variables, such as radiation at the top of the atmosphere (H_0),

showed small oscillations (35.76 ± 2.95 to 36.36 ± 2.55 MJ m⁻² d⁻¹), depending on the local latitudes.

Table 6. Annual averages and standard errors of the averages of the meteorological (Hg, S, Tmax, Tmed, Tmin, RHmed, and rainfall—rainfall of the average annual totals) and astronomical variables (H₀), obtained on a daily scale for the 20 meteorological stations studied in the Brazilian Amazon.

Stations	Hg (MJ m ⁻² d ⁻¹)	H ₀ (MJ m ⁻² d ⁻¹)	Kt	S (hours)	Ri	Tmax (°C)	Tmed (°C)	Tmin (°C)	RHmed (%)	Rainfall (mm year ⁻¹)
1	17.17 ± 4.80	36.23 ± 3.40	0.47 ± 0.13	5.58 ± 3.11	0.46 ± 0.26	31.29 ± 2.84	25.60 ± 2.04	21.68 ± 1.96	78.42 ± 12.52	2954 ± 139
2	19.86 ± 5.28	36.12 ± 1.35	0.55 ± 0.14	6.95 ± 3.23	0.58 ± 0.26	31.76 ± 1.65	27.54 ± 1.22	23.97 ± 0.73	76.56 ± 1.22	2100 ± 145
3	17.17 ± 5.23	35.99 ± 1.34	0.48 ± 0.14	4.77 ± 3.12	0.40 ± 0.08	32.02 ± 2.29	26.34 ± 1.23	22.76 ± 1.18	83.88 ± 6.11	2443 ± 72
4	15.64 ± 4.25	36.36 ± 2.55	0.43 ± 0.12	3.94 ± 2.70	0.33 ± 0.22	31.55 ± 2.27	25.92 ± 1.48	22.24 ± 1.39	70.16 ± 14.29	1952 ± 75
5	16.12 ± 5.09	36.05 ± 1.98	0.45 ± 0.14	5.78 ± 3.33	0.48 ± 0.27	31.52 ± 2.24	27.24 ± 1.44	24.01 ± 0.98	79.57 ± 6.57	2339 ± 104
6	17.15 ± 3.84	35.76 ± 2.95	0.48 ± 0.10	5.24 ± 3.30	0.44 ± 0.25	32.75 ± 2.10	26.70 ± 1.30	22.57 ± 1.51	78.86 ± 5.96	2230 ± 103
7	16.34 ± 5.04	35.91 ± 2.03	0.46 ± 0.14	5.52 ± 3.23	0.46 ± 0.27	32.30 ± 2.21	27.74 ± 1.64	24.32 ± 1.22	75.86 ± 9.16	2206 ± 99
8	17.52 ± 5.41	35.88 ± 1.84	0.49 ± 0.14	6.17 ± 3.41	0.51 ± 0.28	31.29 ± 2.07	27.15 ± 1.43	24.24 ± 1.09	81.09 ± 6.72	2343 ± 110
9	15.22 ± 4.76	36.17 ± 1.30	0.42 ± 0.12	4.73 ± 2.81	0.39 ± 0.23	31.30 ± 2.23	26.41 ± 1.45	23.14 ± 1.19	81.46 ± 7.99	2867 ± 46
10	19.13 ± 4.19	35.95 ± 3.96	0.53 ± 0.12	6.03 ± 3.04	0.50 ± 0.26	32.35 ± 2.81	25.41 ± 1.63	20.16 ± 2.11	72.04 ± 15.78	1952 ± 132
11	15.09 ± 3.59	36.04 ± 1.55	0.42 ± 0.10	6.48 ± 2.75	0.54 ± 0.23	32.67 ± 1.35	27.27 ± 1.09	23.56 ± 0.65	78.49 ± 5.75	3205 ± 129
12	20.16 ± 3.78	35.91 ± 1.79	0.56 ± 0.10	7.57 ± 2.59	0.63 ± 0.21	32.47 ± 1.21	27.75 ± 1.13	24.23 ± 1.02	74.36 ± 6.15	2230 ± 137
13	18.64 ± 4.46	35.79 ± 3.26	0.52 ± 0.13	6.96 ± 3.26	0.58 ± 0.28	33.54 ± 2.75	26.83 ± 1.69	21.60 ± 2.12	70.50 ± 12.26	1686 ± 104
14	18.75 ± 4.71	36.03 ± 2.25	0.52 ± 0.13	6.24 ± 3.18	0.52 ± 0.26	32.67 ± 2.17	27.58 ± 1.46	23.85 ± 0.96	74.87 ± 7.16	2069 ± 95
15	18.25 ± 3.87	35.82 ± 2.57	0.51 ± 0.11	6.36 ± 3.10	0.53 ± 0.26	32.26 ± 1.95	26.59 ± 1.14	22.40 ± 1.37	76.53 ± 7.75	1885 ± 123
16	20.61 ± 4.19	36.13 ± 1.71	0.57 ± 0.11	7.53 ± 2.79	0.63 ± 0.23	31.66 ± 1.69	27.54 ± 1.29	23.97 ± 1.05	75.30 ± 6.98	1661 ± 104
17	16.64 ± 4.52	36.21 ± 2.31	0.46 ± 0.12	6.70 ± 3.21	0.56 ± 0.26	33.08 ± 2.45	26.84 ± 1.46	22.74 ± 0.78	78.22 ± 8.71	2572 ± 107
18	19.82 ± 4.30	35.96 ± 1.38	0.55 ± 0.12	6.89 ± 3.55	0.57 ± 0.29	30.94 ± 0.95	27.71 ± 1.04	25.34 ± 1.51	76.98 ± 6.03	2093 ± 74
19	16.95 ± 3.48	36.06 ± 1.99	0.47 ± 0.09	6.22 ± 2.81	0.52 ± 0.23	31.43 ± 1.68	26.73 ± 1.15	23.36 ± 0.94	78.42 ± 7.70	2400 ± 157
20	19.35 ± 4.35	35.99 ± 1.77	0.54 ± 0.11	6.49 ± 2.87	0.54 ± 0.23	33.51 ± 2.22	27.83 ± 1.56	23.70 ± 1.07	68.54 ± 10.17	1.616 ± 100

Global radiation (Hg, MJ m⁻² d⁻¹), extraterrestrial radiation (H₀, MJ m⁻² d⁻¹), transmissivity coefficient (Hg/H₀), insolation (S, hours), photoperiod (S₀, hours), insolation ratio (S/S₀), maximum temperature (Tmax, °C), average temperature (Tmed °C), minimum temperature (Tmin, °C), average relative humidity (RHmed, %), and rainfall (mm year⁻¹).

When analyzing the correlations between the meteorological variables (Figure 2) together for the 20 meteorological stations, it is observed that, for global radiation, only in the correlation with the mean relative humidity (RHmed) does a decrease in Hg occur with an increase in RHmed; in this case, when adjusting the simple linear regression [Hg = 37.74 – 0.2627 RHmed], a correlation coefficient of –0.52 was obtained. On the other hand, the worst correlations are observed with Tmin (correlation coefficient “r” = 0.081). Weak correlations between Hg and Tmin or RHmax are expected since these two variables are interdependent regarding the times of occurrence (normally at night—an absence of solar radiation). Stronger and increasing correlations of Hg with Tmed and Tmax are also observed, with correlation coefficients of 0.56 and 0.66, respectively; as for the insolation (S) measured in the heliographs, it is found that there is a linear coefficient that indicates the existence of S for minimum Hg values of approximately 2.0 MJ m⁻² d⁻¹, with a correlation coefficient of 0.83 and smaller dispersions.

For the frequency distributions, normal distributions are observed for Tmax, Tmed, and Tmin; for Hg and RHmed, the averages occur in percentiles above 60%. Regarding S, there are higher percentages of cloudy days (S = 0) and an increasing frequency of occurrences between 1 and 11 h of insolation. The Hg interpolations show greater uniformity when associated with Tmax and S. To evaluate the behavior of global radiation throughout the year as a function of the seasonality of rainfall in the Amazon biome, the grouping of monthly data for the 20 meteorological stations was considered, and the values were plotted in boxplots (Figure 3).

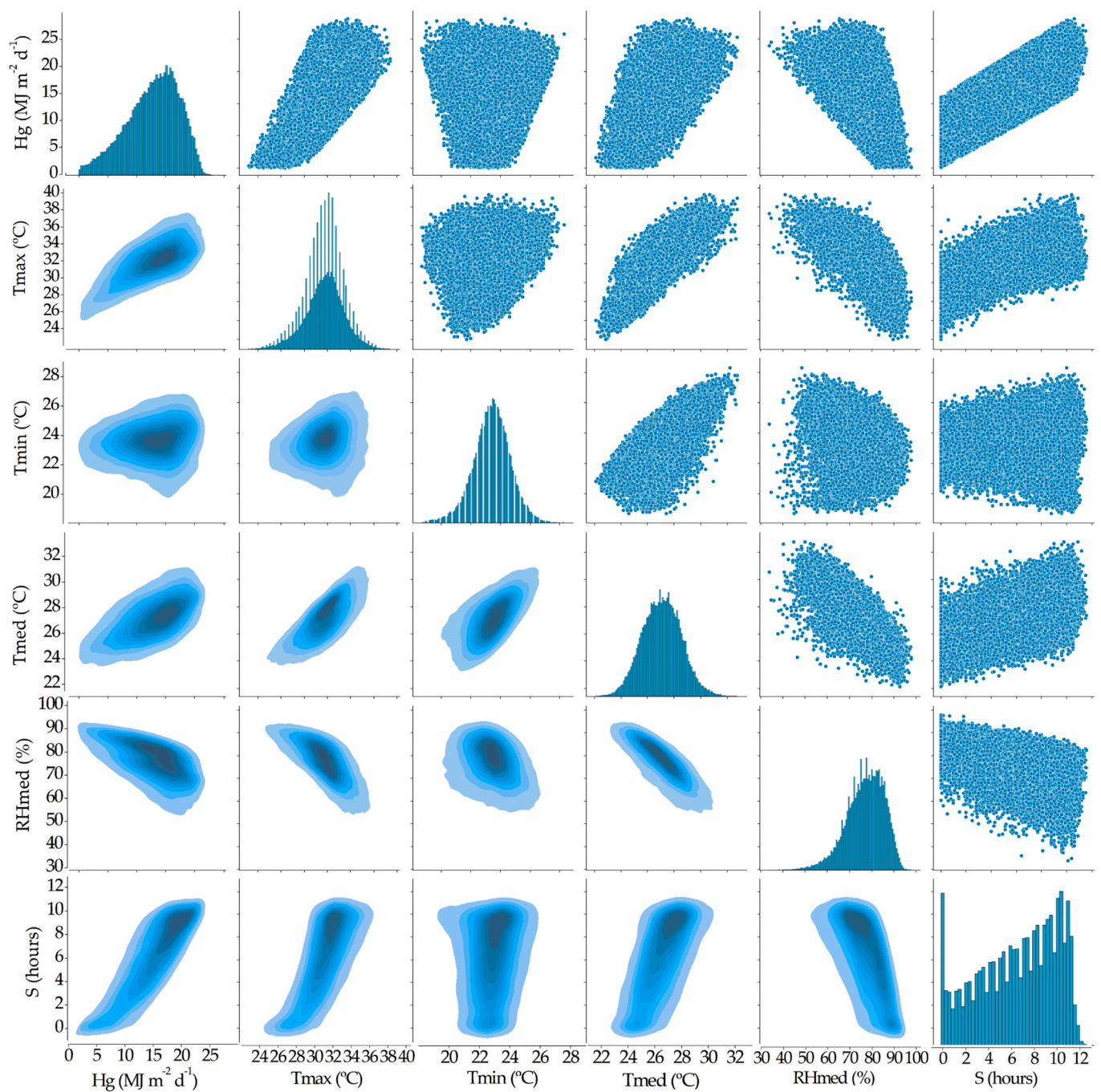


Figure 2. Correlations (points), frequency distributions (diagonal of the frame), and data density (by color scale—the darker, the greater the density of correlated points) between meteorological variables (Hg, Tmax, Tmin, Tmed, RHmed, and S) in the Brazilian Amazon biome.

Although many meteorological stations are located at close latitudes, the average global radiation incidence can vary significantly among themselves; for example, at the meteorological stations of Macapá (0.035° N), Barcelos (-0.98° S), and São Gabriel da Cachoeira (-0.12° S), where the median Hg values were 21.52 , 18.09 , and 15.79 $\text{MJ m}^{-2} \text{d}^{-1}$, respectively, this behavior shows the influence of precipitation (cloudiness) on Hg, since, at these meteorological stations, the annual rainfall totals are 2100 , 2433 , and 2867 mm, respectively. It is also possible to consider in the comparison between these same three meteorological stations that the effect of the proximity of large surfaces of free water (as occurs in Macapá) is that the incidence of Hg depends on the movements of regional or

mesoscale atmospheric circulation. On water-free surfaces, there may be a potential increase in actual water vapor pressures (e_a) in the atmosphere, due to higher levels of direct water evaporation. However, this water vapor can be transported in the atmosphere to other regions by winds, thus reducing the attenuation of water vapor in Hg on a local scale.

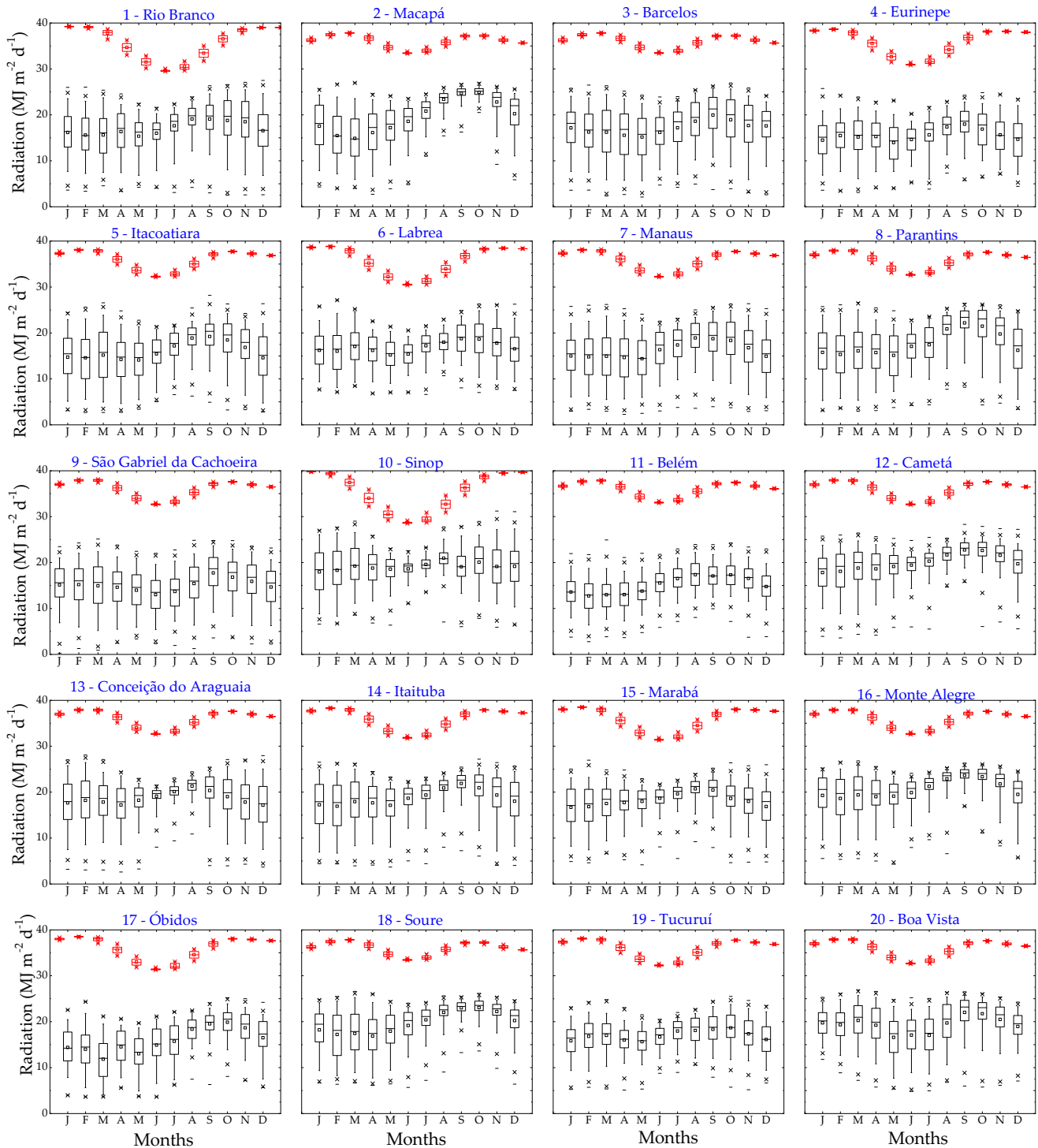


Figure 3. Monthly boxplots of measured daily global radiation (H_g —black lines and markers) and calculated extraterrestrial radiation (H_0 —red lines and markers) monthly for 20 meteorological stations in the Brazilian Amazon (for each cluster of monthly data, the median, mean, maximum, and minimum limits of the daily values are represented).

In the rainy season (October to April), Hg averages are generally lower compared to the dry season (May to September) in the region. It is worth noting that the minimum values of global radiation as an outlier in the rainy season for most of the EMAs evaluated are related to the presence of clouds. However, they can also occur in the dry season when associated with fires, common in the region during this period. They emit particulate matter that remains suspended in the atmosphere, thus attenuating Hg through absorption and non-selective diffusion and reducing atmospheric transmissivity.

Another way to observe the variations of Hg in the Brazilian Amazon can be performed between meteorological stations located at different latitudes of the biome (Figure 4) by comparing the daily seasonality of Hg throughout the analyzed period for the meteorological stations of Boa Vista (2.82° N), Manaus (3.10° S), and Sinop (11.85° S). It is noted that in Sinop the maximum Hg reached close to 30 MJ m⁻² d⁻¹. There is less variation in the daily averages in the dry season than in the rainy season. Furthermore, as the time of year influences extraterrestrial radiation (H₀), it is clear that, in the dry season, due to the solar declination and the latitude of Sinop, the daily H₀ values are lower, and, consequently, they can generate higher atmospheric transmissivity coefficients when compared to other meteorological stations in the biome.

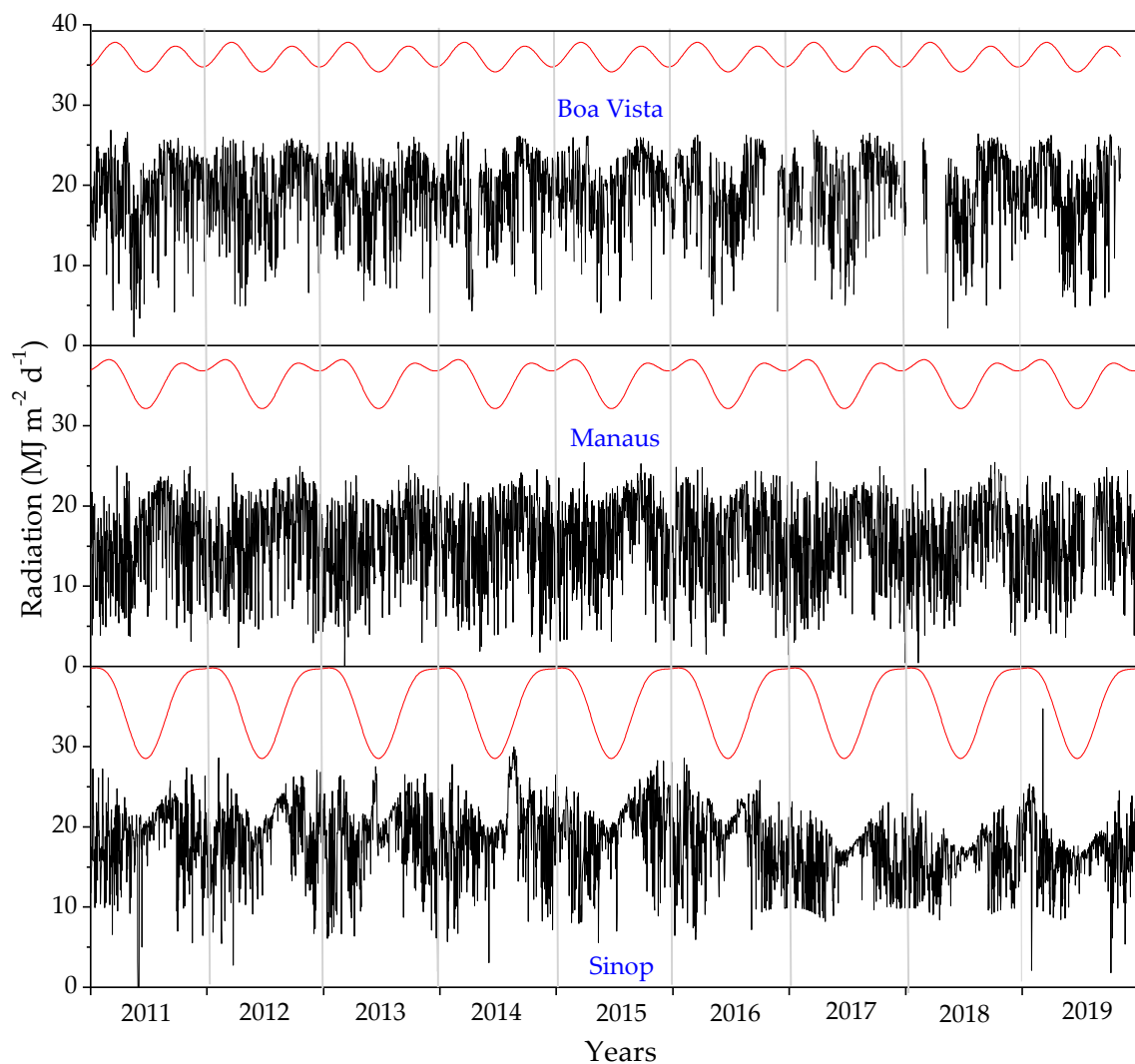


Figure 4. Variation of daily global (Hg—black lines) and extraterrestrial (H₀—red lines) radiation for Boa Vista, Manaus, and Sinop meteorological stations in the Brazilian Amazon over different years of measurements.

Each simplified Hg estimation model’s specific coefficients (a, b, c, and d) were calibrated using the Statistica 14.0.0.15 software. By using the *t*-test at a significance level of 5%, the significance of the adjusted coefficients for each model was verified. The values of the adjusted coefficients for the best models in the 20 meteorological stations evaluated can be found in Table 7. The results of the statistical performance indicators (MBE, RMSE, and Willmott’s “d”) were presented only for the models with adjusted coefficients that were significant at 5%.

Table 7. Calibrated coefficients for models 10, 45, and 62 of estimates of daily global radiation for each meteorological station evaluated in the Brazilian Amazon biome.

Met. Stations	Model 10				Model 62				
	a	b	c	R ²	a	b	c	d	R ²
1	0.2122	0.4784	0.7003	0.772	0.0324	0.1163	0.3607	0.8035	0.8052
2	0.1995	0.538	0.7178	0.8958	0.0396	0.1123	0.4516	0.8104	0.9071
3	0.2142	0.4846	0.5639	0.8045	0.0351	0.1127	0.3832	0.6435	0.8262
4	0.2233	0.4343	0.5737	0.758	-	-	-	-	-
5	0.1817	0.4678	0.6911	0.8221	0.0479	0.0936	0.3885	0.7413	0.8376
6	0.2769	0.3842	0.6852	0.7606	0.1265	0.0815	0.3178	0.683	0.7777
7	0.2041	0.4737	0.7516	0.7846	0.0518	0.0969	0.4094	0.8466	0.7992
8	0.1672	0.527	0.6562	0.8933	0.0733	0.0728	0.4662	0.7124	0.9003
9	0.1825	0.4718	0.6701	0.7713	−0.0453	0.1738	0.2741	0.9689	0.8673
10	0.3103	0.4191	0.852	0.6359	0.1515	0.0821	0.3388	0.8233	0.665
11	0.2171	0.3681	0.9748	0.6563	0.0794	0.0846	0.3203	1.25	0.6658
12	0.2159	0.4893	0.7101	0.8452	0.1109	0.0687	0.4474	0.7844	0.852
13	0.197	0.494	0.6848	0.8221	0.1327	0.041	0.4448	0.6997	0.8263
14	0.2113	0.494	0.6286	0.887	0.1042	0.0718	0.4294	0.6683	0.8954
15	0.2355	0.4382	0.6629	0.8081	0.0935	0.0862	0.36	0.6808	0.8256
16	0.2055	0.5173	0.6947	0.9029	0.1331	0.0499	0.4823	0.7233	0.9068
17	0.1968	0.4229	0.7587	0.794	0.0487	0.0876	0.3483	0.8363	0.8065
18	0.278	0.4029	0.6001	0.8422	0.2053	0.045	0.4053	0.6424	0.8477
19	0.2549	0.3692	0.778	0.6905	0.123	0.0836	0.3203	0.9069	0.7108
20	0.2453	0.4656	0.7138	0.8429	0.1176	0.0766	0.4036	0.7679	0.8503

Met. Stations	Model 45					
	a	b	c	d	e	R ²
1	7.1	−0.413	−13.02	6.47	0.3146	0.6513
2	18.05	−1.06	−32.94	16.11	1.08	0.7264
3	6.68	−0.3971	−13.03	6.39	1.04	0.7197
4	4.56	−0.2595	−8.59	4.26	0.4144	0.6825
5	12.48	−0.7875	−23.28	11.62	0.7932	0.7007
6	10.72	−0.5403	−18.54	8.83	0.3082	0.6095
7	14.57	−0.8666	−26.66	13.08	0.8747	0.6124
8	13.14	−0.9469	−25.69	13.19	1.17	0.7341
9	1.52	−0.0997	−3.45	1.84	0.4104	0.8
10	7.33	−0.3692	−12.76	6.12	0.2696	0.4998
11	13.04	−0.6702	−22.98	10.87	0.8086	0.4661
12	-	-	-	-	-	-
13	2.93	−0.2	−6.02	3.16	0.3889	0.629
14	13.7	−0.8282	−25.04	12.42	0.5538	0.6981
15	5.06	−0.3339	−9.95	5.1	0.4996	0.6639
16	27.61	−1.71	−50.07	24.76	1.09	0.6741
17	13.64	−0.6925	−23.86	11.31	0.5745	0.6767
18	−33.41	1.81	55.84	−26.79	1.72	0.3738
19	-	-	-	-	-	-
20	11.07	−0.5971	−20.36	9.72	1.17	0.7435

The statistical performance of the empirical models was represented in boxplots, grouping all the meteorological stations (Figure 5). Analyzing the models in group I, more

significant improvements need to be made when comparing the polynomial changes of the traditional Angstrom–Prescott model (model 1). Overall, for this group, the values of the coefficient of determination (R^2), relative error (MBE), spread (RMSE), and fit (d) were, on average, 0.7780, $-0.01 \text{ MJ m}^{-2} \text{ d}^{-1}$, $2.09 \text{ MJ m}^{-2} \text{ d}^{-1}$, and 0.9310, respectively. In this group, model 11 [$\text{Hg}/\text{H}_0 = a(1/(f(S)/S_0))$] presented the worst statistical performances, with the R^2 , MBE, RMSE, and average d being 0.4980, $-0.329 \text{ MJ m}^{-2} \text{ d}^{-1}$, $3.34 \text{ MJ m}^{-2} \text{ d}^{-1}$, and 0.9140, respectively. Furthermore, when comparing the models that present the same analytical basis, it is observed that model 10 [$\text{Hg}/\text{H}_0 = a + b(S/S_0)^c$] presented a superior statistical performance to the remaining models dependent on insolation (S) with the R^2 , MBE, RMSE, and average d being 0.7990, $0.017 \text{ MJ m}^{-2} \text{ d}^{-1}$, $1.95 \text{ MJ m}^{-2} \text{ d}^{-1}$, and 0.9400.

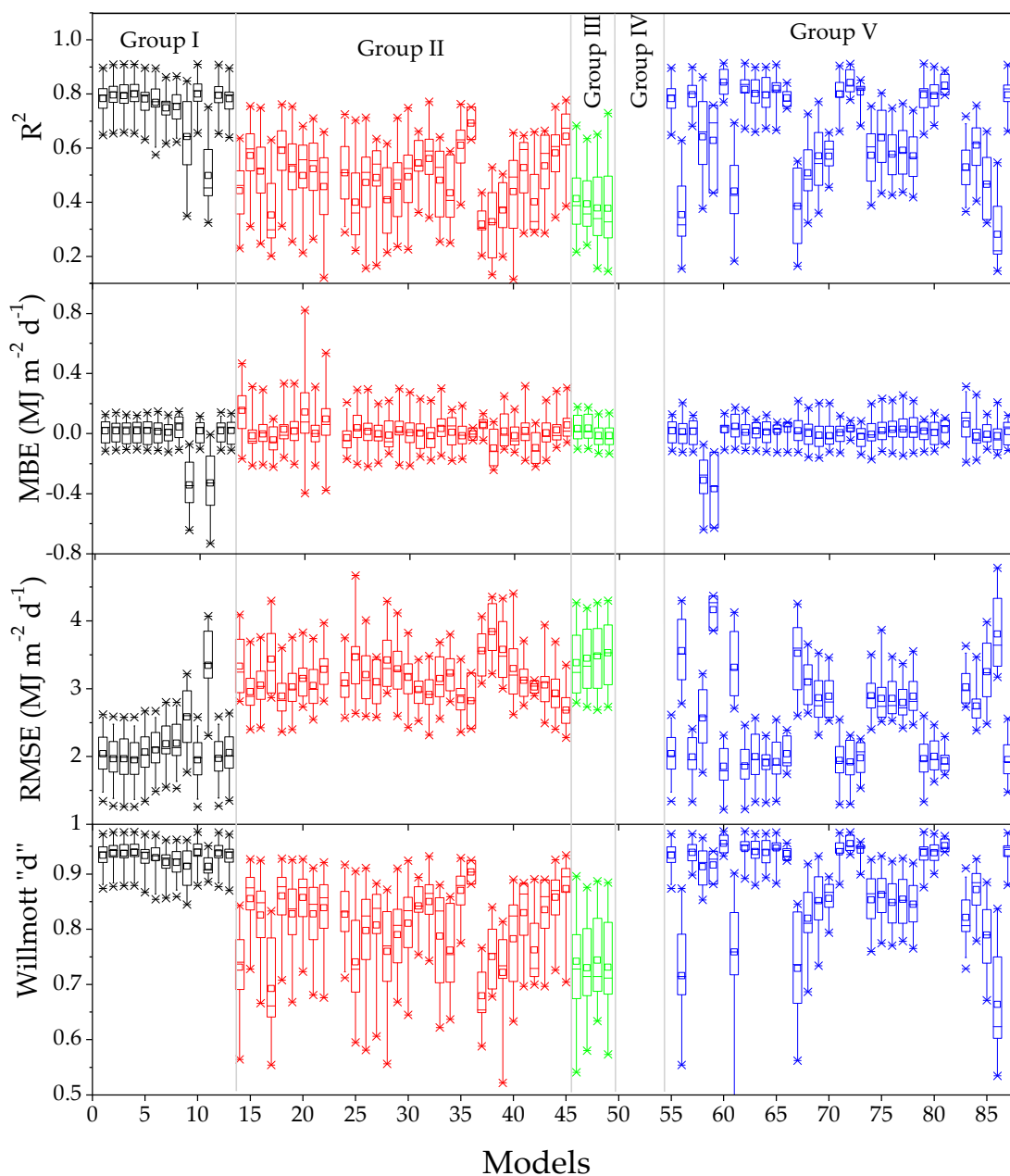


Figure 5. Boxplots of statistical performance indicators (R^2 , MBE, RMSE, and d) for 87 simplified Hg estimation models, considering the grouped values of 20 meteorological stations of the Brazilian Amazon biome. Coefficient of determination, R^2 ; mean bias error, MBE; root mean square error, RMSE; and Willmott's concordance index, d (for each boxplot of each model, the median, mean, maximum, and minimum limits of the daily values are represented).

Regarding the simplified models of group II (based on air temperature), model 23 [$Hg/H_0 = a + b * T_{min}$] was dependent only on T_{min} , and H_0 was NS for all the meteorological stations evaluated. This behavior is expected because the minimum air temperature is not simultaneous with the incidence of solar radiation. Model 24 [$Hg/H_0 = a + b * T_{max}$], dependent on T_{max} and H_0 , was the only model with significant coefficients in all the meteorological stations evaluated; however, it did not present the best statistical performance indicators on average. In general, of the 32 models evaluated in this group (involving air temperature), model 17 [$Hg/H_0 = a + b/H_0 + cT_{med}/H_0$] represented the worst statistical performance, with an R^2 , MBE, RMSE, and Wilmott's d average of 0.3520, 0.099 $MJ m^{-2} d^{-1}$, 3.43 $MJ m^{-2} d^{-1}$, and 0.6930, respectively; model 45 [$Hg/H_0 = a + b\Delta T + c\Delta T^{0.25} + d\Delta T^{0.5} + e(T_{med}/H_0)$] presented the best performance with an R^2 , MBE, RMSE, and average d of 0.6430, 0.056 $MJ m^{-2} d^{-1}$, 2.68 $MJ m^{-2} d^{-1}$, and 0.8730. However, these models did not present significant adjustments for the meteorological stations located in Cametá and Tucuú.

Empirical models that employ the thermal amplitude [$\Delta T = T_{max} - T_{min}$] as an input variable present a better estimate. Comparing the performance of model 14 [$Hg/H_0 = a\Delta T^{0.5}$] and model 16 [$Hg/H_0 = a + b\Delta T^{0.5}$], it is observed that the insertion of the linear coefficient significantly improves the statistical performance, since the R^2 values varied from 0.4420 to 0.5150, with a reduction in the MBE from 0.154 to $-0.003 MJ m^{-2} d^{-1}$ and in the RMSE from 3.33 to 3.05 $MJ m^{-2} d^{-1}$ and also with an increase in the adjustment index (d) from 0.7312 to 0.8257.

The simplified models of group III (based only on the average daily relative humidity— RH_{med}) did not present significant coefficients by the t-test at the meteorological stations of Eirunepé, São Gabriel da Cachoeira, and Sinop. As a rule, the statistical performances of the models in group III were worse when compared to the models in the other groups. In this case, the best estimates in this group were generated by model 46 [$Hg/H_0 = a/H_0 + b(RH_{med}/H_0)$], with R^2 , MBE, RMSE, and d values of 0.4130, 0.034 $MJ m^{-2} d^{-1}$, 3.38 $MJ m^{-2} d^{-1}$, and 0.7420, respectively. As for the models in group IV (based on astronomical variables), none presented statistical significance for any of the meteorological stations evaluated. In group V (the hybrid models), the best estimates of Hg were generated by model 62 [$Hg/H_0 = a + b\ln\Delta T + c(S/S_0)^d$], with mean values of R^2 , MBE, RMSE, and d of 0.8170, 0.008 $MJ m^{-2} d^{-1}$, 1.86 $MJ m^{-2} d^{-1}$, and 0.9460, respectively.

Considering only the models that presented the best statistical performances in each group (Figure 6), it is observed that, in most meteorological stations, the best Hg estimates were generated by models 62 and 10. In this case, model 62 presented values ranging from 0.6714 to 0.9137 for R^2 , from -0.112 to 0.154 $MJ m^{-2} d^{-1}$ for MBE, from 1.22 to 2.46 $MJ m^{-2} d^{-1}$ for RMSE, and from 0.8921 to 0.9772 for the adjustment index (d). Model 10 presented variations in R^2 from 0.6549 to 0.9091, MBE from -0.103 to 0.115 $MJ m^{-2} d^{-1}$, RMSE from 1.26 to 2.58 $MJ m^{-2} d^{-1}$, and the “ d ” index from 0.8793 to 0.9760.

The main difference between the input variables of these two models is the addition of the Napierian logarithm (\ln) in the thermal amplitude ($T_{max} - T_{min}$) in model 62, which did not significantly improve the model's predictive capacity. However, it is noteworthy that these two models (62 and 10) are based on sunlight; therefore, in cases of minimum data availability, model 45, which depends only on air temperature, should preferably be used since it generates better responses than the models associated with relative humidity.

Figure 7 presents the dispersions of Hg measured and estimated by models 10, 45, and 62 for the three aforementioned meteorological stations that represent the latitude variation in the Amazon biome (Boa Vista, Manaus, and Sinop). In this case, four different classes of atmospheric transmissivity were considered, which represent the conditions of a cloudy sky ($0 < Kt < 0.35$), partly cloudy with a predominance of diffuse radiation ($0.35 < Kt < 0.55$), partly open with a predominance of direct radiation ($0.55 < Kt < 0.65$), and an open sky

($K_t > 0.65$), as recommended by Escobedo et al. [73] and Souza et al. [15]. Almost always, the global radiation estimated by models 10 and 62 were similar and followed close to the reference line (1:1), with a greater dispersion of the estimated values when K_t was below 0.55.

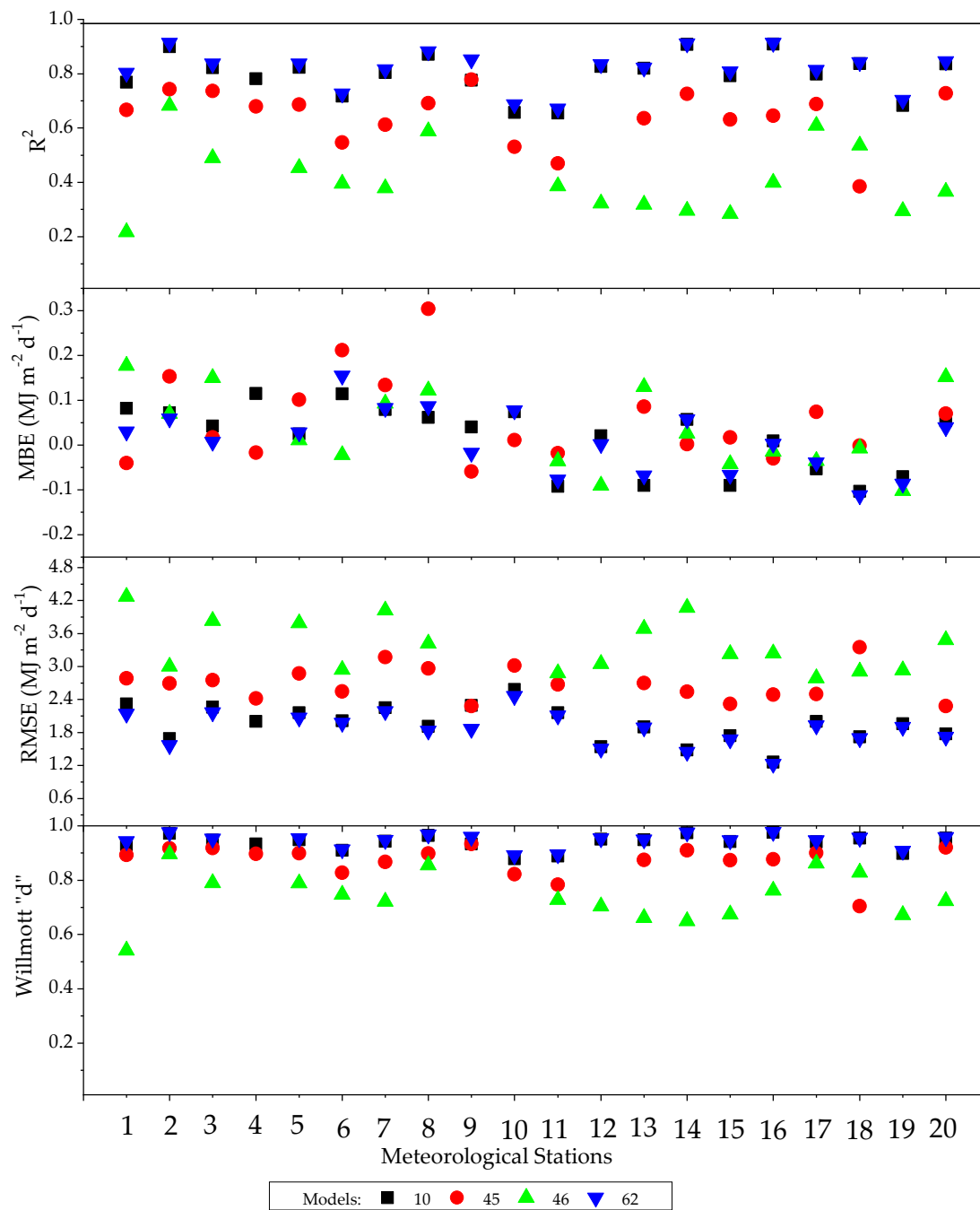


Figure 6. Statistical performance indicators of each group’s best simplified estimation models (models 10, 45, 46, and 62) for 20 meteorological stations of the Brazilian Amazon biome. Coefficient of determination, R^2 ; mean bias error, MBE; root mean square error, RMSE; and Willmott’s concordance index, d .

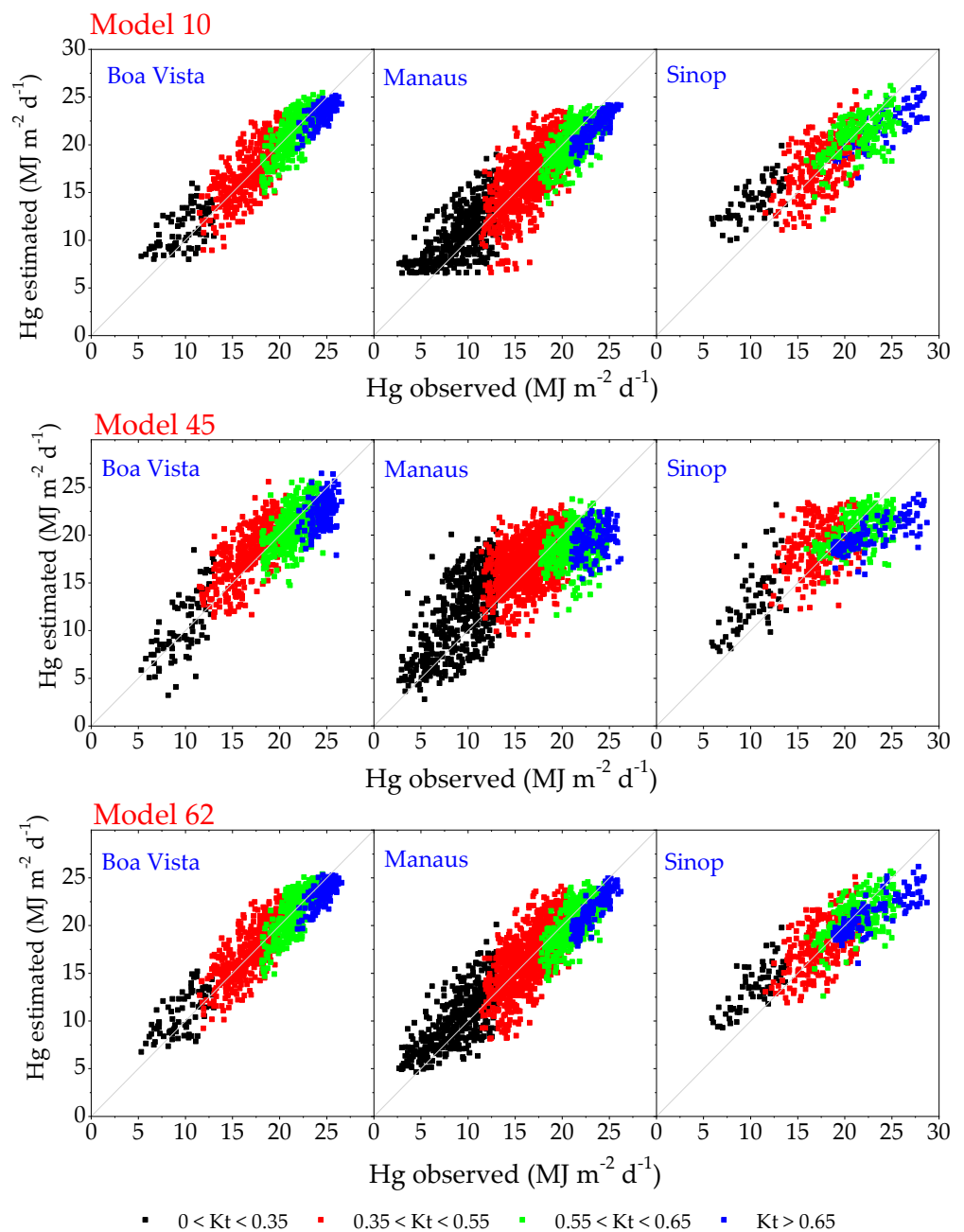


Figure 7. The dispersion between the global radiation measured and estimated by models 10, 45, and 62 for the meteorological stations of Boa Vista (RR), Manaus (AM), and Sinop (MT) in different classes of atmospheric transmissivity. The gray line represents the relationship 1:1 or $y = x$.

The absolute accumulated errors in the frequency of occurrence (Figure 8) up to the value of $2.0 \text{ MJ m}^{-2} \text{ d}^{-1}$ in the Hg estimate using models 10, 45, and 62 at the meteorological stations of Boa Vista and Sinop was 84, 83, and 85% and 67, 68, and 68%, respectively; however, in Manaus, there was a significant difference in the values, with values of 75, 64, and 82%. Depending on the city evaluated, the frequency of the accumulated error up to $2.0 \text{ MJ m}^{-2} \text{ d}^{-1}$ can be high (Boa Vista) or low (Sinop); that is, local meteorological conditions directly influence the error.

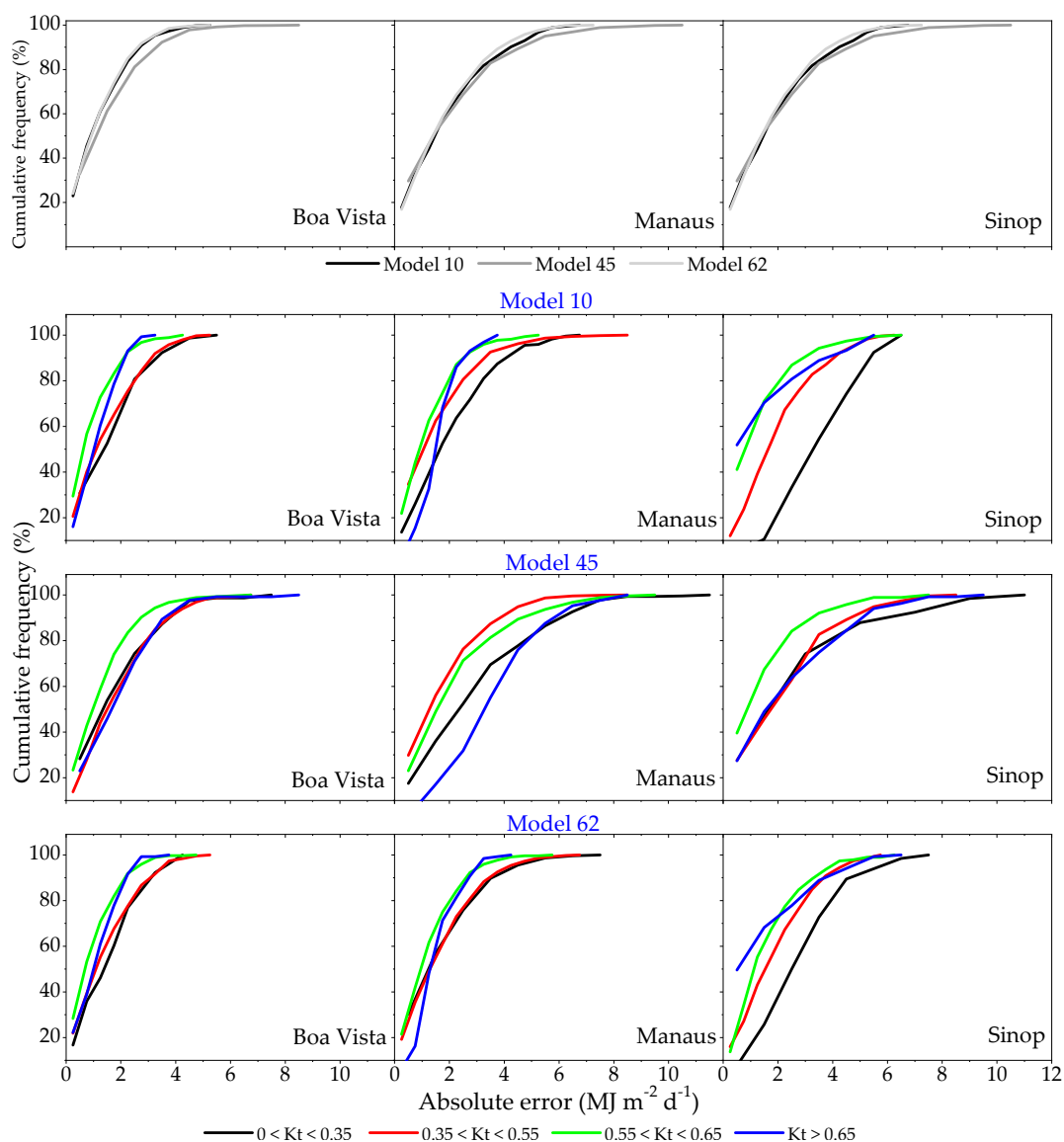


Figure 8. Absolute error frequency at the meteorological stations of Boa Vista, Manaus, and Sinop for models 10, 45, and 62 and different atmospheric transmissivities.

The reduction in the accumulated absolute error by up to $2.0 \text{ MJ m}^{-2} \text{ d}^{-1}$ in meteorological conditions of low atmospheric transmissivity ($0 < Kt < 0.35$) is more efficient in hybrid model 62 (55 to 85%) when compared to model 10 (33 to 80%) and model 45 (38 to 74%), following the same trend in the meteorological conditions of high atmospheric transmissivity ($Kt > 0.65$), with accumulated frequencies for model 62 of 82 to 93%, model 10 of 78 to 87%, and model 45 of 32 to 71%. In the condition of partially cloudy skies with a predominance of diffuse radiation ($0.35 < Kt < 0.55$), when comparing model 10 (67 to 81%) and model 62 (67 to 79%), there was no difference in the accumulated error; however, model 45 (60 to 70%) had the greatest possibility of errors above $2.0 \text{ MJ m}^{-2} \text{ d}^{-1}$. This pattern was repeated in the condition of partially open skies with a predominance of direct radiation ($0.55 < Kt < 0.65$) with model 10 (87 to 93%), model 62 (88 to 92%), and model 45 (71 to 84%).

To allow the applications and estimates of Hg, the adjusted coefficients are presented only for these three simplified models (10, 45, and 62), in the 20 meteorological stations evaluated in the Amazon biome (Table 7). The calibrated coefficients for each model and weather station are presented as supplementary materials to the article. In some cities, models

45 and 62 were NS (not significant). For group II (based on air temperature), model 65 is recommended for the cities of Cametá [$\text{Hg} = (-0.0942 + (-0.2688 + 0.0179T_{\text{med}})\Delta T^{0.5})H_0$] and Tucuruí [$\text{Hg} = (0.0655 + (-0.1478 + 0.0108T_{\text{med}})\Delta T^{0.5})H_0$], and, in group V (the hybrid combination), model 72 presented the best performance for the city of Eirunepé [$\text{Hg} = (-0.0947 - 0.0077T_{\text{min}} + 0.0188T_{\text{max}} + 0.3163(S/S_0))H_0$].

4. Discussion

The results found in this study provide details of the local calibration and statistical significance of the coefficients of 87 models for the daily estimation of global radiation in tropical climate regions, having as input variables meteorological data that can easily be made available by routine measurements at meteorological stations. Determining the significance of the coefficients of each model is relevant information in the modeling since the lower P-value of the t-test at the α significance level (5%) indicates that, in the region evaluated, the meteorological and environmental conditions may be complex and cause greater uncertainties in the Hg estimate [35]. This can be observed by the large number of models with locally calibrated NS coefficients. As observed in Figures 2–4, insolation (S) and global radiation (Hg) incidence in the Amazon biome are significantly influenced by atmospheric components, such as the emission of aerosols into the atmosphere through the burning of vegetation in the dry season of the Amazon basin [19] or the presence of clouds due to high rainfall in the rainy season [63,74].

These conditions are the main factor in attenuating Hg and the increase in uncertainty in the insolation values due to the sensitivity to heliograph burning and maintenance. According to the results (Figure 5), the best statistical performance was obtained by modifying the Angstrom–Prescott linear model to a model that uses power in its explanatory variable [$\text{Hg}/H_0 = a + b(S/S_0)^c$]. According to Almorox and Hontoria [34] and Bakirci [35], depending on the atmospheric transmissivity conditions, the relationship between S and Hg can be better represented by linear, polynomial, logarithmic, exponential, or hybrid correlations. For Santos et al. [30], even in conditions where there is an absence of cloudiness (an open sky), the elements present in the Earth’s atmosphere can attenuate solar radiation by diffusion (scattering) and influence Hg.

When evaluating the different models of group I under the climatic conditions of Turkey, Bakirci [35] did not observe significant differences in the statistical performances of the linear, exponential, and logarithmic models, obtaining coefficients of determination (R^2) greater than 0.96, MBE values ranging from 0.20 to 0.24 $\text{MJ m}^{-2} \text{d}^{-1}$, and RMSE values from 1.31 to 1.35 $\text{MJ m}^{-2} \text{d}^{-1}$. Almorox and Hontoria [34], in sixteen cities in Spain, evaluated linear and polynomial models of the second- and third-degree, as well as logarithmic and exponential models, based on insolation (S), and concluded that all statistical models could be used to estimate Hg with good precision; however, they recommended the linear model due to its simplicity and because it presents a better statistical performance.

It was observed that the performance of models 8, 9, and 11, which do not have a linear coefficient (a), was lower in all cities. According to Prieto and García [11], this coefficient represents the minimum transmissivity of the region’s atmosphere and is associated with diffuse radiation. In the Amazon, this condition represents a considerable part of global radiation due to the seasonality of rainfall and changes in the composition of the atmosphere [15], and, therefore, models that do not present coefficients that characterize days with low atmospheric transmissivity can generate larger errors for adjustments in annual or seasonal groupings; in cases of monthly adjustments, these models can potentially present good estimates for dry months (with an absence of cloudiness) in some regions of the Amazon.

Nevertheless, regarding interference, in some regions, climate change can increase precipitation, which results in a reduction in atmospheric transmissivity and, consequently, in the adjustment of models, as is the case in the city of Boa Vista, where, according to Araújo et al. [74], analyzing the period of meteorological data from 1961 to 2020 and the

variations between the two climatological models, there was an increase in precipitation from 1420.4 to 1761.8 mm year⁻¹ and in the average air temperature from 27.4 to 28.2 °C.

For the group II models (based on air temperature), the best estimates of daily global radiation were obtained with a certain model [$H_g/H_0 = a + b(T_{max} - T_{min}) + c(T_{max} - T_{min})^{0.25} + d(T_{max} - T_{min})^{0.5} + e(T_{med}/H_0)$], corroborating the results found by Qiu et al. [1]. These authors evaluated 78 models based on air temperature for 105 meteorological stations in China and concluded that models that relate thermal amplitude [$\Delta T = T_{max} - T_{min}$] and maximum, mean, and minimum temperatures (T_{max} , T_{med} , and T_{min}) present better estimates. In models based on air temperature, ΔT is related to several local factors that directly influence the radiation and energy balance, such as latitude, rainfall, current water vapor pressure, atmospheric transmissivity (cloudiness), and proximity to large free water surfaces, among other factors [30]. This is an essential parameter in models based only on air temperature when the aim is to improve predictive capacity, since ΔT has a good correlation with H_g [1].

It is also worth noting that the statistical performance of the empirical models of groups I and II in estimating H_g in the Amazon can be considered satisfactory. Sometimes, depending on the study region and the input variables, an empirical model may present a variable performance depending on the climatic conditions of the region; for example, in this study under tropical conditions, model 37 [$H_g/H_0 = a + bH_0Tm^c$] presented the worst performance in group II with coefficients of determination ranging from 0.2765 to 0.4000. In these cases, the adjusted coefficients were insignificant in 55% of the meteorological stations evaluated. However, for the Cairo region (Egypt) with its dry and desert climate, Hassan et al. [12], evaluating 20 models based on air temperature, found that this same model (37) presented the best statistical performance in daily H_g estimates, with an RMSE of 0.5813 MJ m⁻² d⁻¹ and an R² of 0.9897.

The significance of regionally calibrated empirical models can be considered the combination of two factors: the first related to the input meteorological variables representing the location's environmental conditions, and the second due to the empirical model's structure. The lowest performances in the estimation of H_g were obtained with the empirical models based on relative humidity (group III). The group III models generally presented good estimates in arid regions with low annual rainfall totals, such as Nigeria [29,49], Bahrain [39], and Turkey [55].

The five models in group IV were NS for all 20 meteorological stations evaluated. The astronomical input variables, such as solar declination, photoperiod, and Julian day, are variables that do not consider local factors related to atmospheric and geographic conditions, which can directly interfere with global radiation incidence on the surface, where the use of radiometric fractions aims to minimize these effects [15,73]. Group IV models are used in countries with arid regions, low rainfall, and high atmospheric transmissivity, such as Saudi Arabia [50] and Jordan [56]. Although the statistical performances of hybrid models (group V) are better when compared to simplified models with air temperature (group II) and relative humidity (group III), these differences are reduced when compared to models based on insolation (group I) (Figure 6). Several studies report considerable differences in the performance of simplified models compared to hybrid models in different climatic regions [2,9–11,21,30].

When analyzing the variations in estimates at meteorological stations at different latitudes in the Amazon (Figure 7), it is again observed that, in general, the models have greater difficulty in estimating days and times of the year with intermediate atmospheric transmissivity (partly cloudy or partially clear skies). According to Santos et al. [30], different combinations of cloud cover can result in the same ΔT value, but each combination of cloud cover results in a single H_g value.

Another point to be highlighted is that using models based on air temperature generally leads to overestimations of H_g [2,10,23,30]. This behavior occurs because air temperature depends on surface heating processes, energy balance, and heat transport, which,

in turn, can reflect levels of sensible heat higher than those that would potentially be generated exclusively by Hg incidence.

Models 10, 45, and 62 presented consistencies in Hg estimates, each with its input variables (from the groups). Due to the spatial distribution of the 20 meteorological stations evaluated, they can be used in the Brazilian Amazon. Despite the good adjustments of the empirical models found in this work, according to Prieto and García [11], after reviewing articles published in the last 100 years on this topic, they found that none of the 165 empirical models with different input variables were consistent and presented good performances in the different climatic regions. This becomes more worrying with climate change scenarios, which predict rising air temperatures and changes in rainfall patterns and gas concentrations, which will directly interfere with the radiation balance [2,18]. This climate change scenario has also been observed in the Amazon biome region, with increased rainfall and air temperature [74,75]. Therefore, it is essential to understand and make available as many models for estimating meteorological variables as possible, allowing regional calibrations and applications in large databases to fill gaps and generate long and consistent databases.

Finally, the empirical models must be recalibrated when these climate change conditions materialize. New studies, mainly in smaller data groups (seasonal and monthly), must be conducted to update the coefficients and maintain the predictive capacity of the different empirical models.

5. Conclusions

The most accurate empirical models for estimating global radiation (Hg) for the Brazilian Amazon biome were, first, the hybrid model based on insolation and air temperature, represented by $[Hg/H_0 = a + b\ln\Delta T + cS/S_0^d]$, followed by the model based on insolation $[Hg/H_0 = a + bS/S_0^c]$, and, finally, the model based on air temperature $[Hg/H_0 = a + b\Delta T + c\Delta T^{0.25} + d\Delta T^{0.5} + eT_{med}/H_0]$.

It is not recommended to use simplified models based solely on relative humidity or astronomical variables to estimate Hg in the Amazon in annual data groupings; these models may present better statistical performances if they are locally calibrated for meteorological stations with well-defined dry and rainy seasons.

Cloudiness and rainfall seasonality affect atmospheric transmissivity and estimates of global radiation. In this case, future updates of these analyses should consider the models that generated the best estimates and seek analyses in seasonal (year or water seasons) and monthly database groupings. The recommendation of simplified models that produce good Hg estimates will also allow comparisons with other methodologies, such as machine learning and reanalysis.

Therefore, generating conditions that bring about the knowledge of global radiation will contribute to numerous agricultural and environmental applications, providing a comprehensive context for applying these estimates on larger spatial and temporal scales.

Supplementary Materials: The following supporting information can be downloaded at <https://www.mdpi.com/article/10.3390/atmos15111397/s1>, Tables S1–S87—adjusted coefficients for each simplified model and statistical performance indicators for the 20 meteorological stations evaluated.

Author Contributions: Conceptualization, C.C.M. and A.P.d.S.; methodology, C.C.M., D.R.B., F.T.d.A., J.G.R.D. and A.P.d.S.; software, C.C.M., R.S.D.P. and D.C.; validation, C.C.M., R.S.D.P. and D.C.; formal analysis, C.C.M., R.S.D.P. and D.C.; investigation, C.C.M., R.S.D.P., D.C., D.R.B., J.G.R.D. and A.P.d.S.; resources, A.P.d.S.; data curation, C.C.M. and A.P.d.S.; writing—original draft preparation, C.C.M.; writing—review and editing, D.R.B., F.T.d.A., J.G.R.D. and A.P.d.S.; visualization, D.R.B., F.T.d.A., J.G.R.D. and A.P.d.S.; supervision, A.P.d.S.; project administration, A.P.d.S.; and funding acquisition, D.R.B., F.T.d.A. and A.P.d.S. All authors have read and agreed to the published version of the manuscript.

Funding: This research was funded by Coordenação de Aperfeiçoamento de Pessoal de Nível Superior—Brazil (CAPES)—finance code 001 and post-doctoral scholarship (Process 88887.946681/2024-00); the National Council for Scientific and Technological Development (CNPq)—process 303522/2022-4; and the Foundation for Research Support of Mato Grosso State (FAPEMAT)—research project process 0182944/2017.

Institutional Review Board Statement: Not applicable.

Informed Consent Statement: Not applicable.

Data Availability Statement: The automatic weather station (AWS) data used in this study can be accessed by the Instituto Nacional de Meteorologia (INMET) databank website: <https://bdmep.inmet.gov.br/#> (accessed on 13 May 2024).

Acknowledgments: The authors also thank all the students of the “Tecnologia em Recursos Hídricos no Centro-Oeste” (dgp.cnpq.br/dgp/espelhogrupo/2399343537529589, accessed on 13 May 2024) and “Interações Ambiente e Planta” research groups (dgp.cnpq.br/dgp/espelhogrupo/1262367131753850, accessed on 13 May 2024). At the Instituto Nacional de Meteorologia (INMET).

Conflicts of Interest: The authors declare no conflicts of interest.

References

1. Qiu, R.; Li, L.; Wu, L.; Agathokleous, E.; Liu, C.; Zhang, B.; Luo, Y.; Sun, S. Modeling daily global solar radiation using only temperature data: Past, development, and future. *Renew. Sustain. Energy Rev.* **2022**, *163*, 112511. [[CrossRef](#)]
2. Samanta, S.; Banerjee, S.; Patra, P.K.; Sehgal, V.K.; Chowdhury, A.; Kumar, B.; Mukherjee, A. Projection of future daily global horizontal irradiance under four RCP scenarios: An assessment through newly developed temperature and rainfall-based empirical model. *Sol. Energy* **2021**, *227*, 23–43. [[CrossRef](#)]
3. Kumler, A.; Kravitz, B.; Draxl, C.; Vimmerstedt, L.; Benton, B.; Lundquist, J.K.; Martim, M.; Buck, H.J.; Wang, H.; Lennard, C.; et al. Potential effects of climate change and solar modification on renewable energy resources. *Renew. Sustain. Energy Rev.* **2025**, *207*, 114934. [[CrossRef](#)]
4. de Souza, A.P.; Zamadei, T.; Borella, D.R.; Martim, C.C.; de Almeida, F.T.; Escobedo, J.F. Diurnal evolution and estimates of hourly diffuse radiation based on horizontal global radiation, in Cerrado-Amazon Transition, Brazil. *Atmosphere* **2023**, *14*, 1289. [[CrossRef](#)]
5. Luo, H.; Han, Y.; Lu, C.; Yang, J.; Wu, Y. Characteristics of Surface Solar Radiation under Different Air Pollution Conditions over Nanjing, China: Observation and Simulation. *Adv. Atmos. Sci.* **2019**, *36*, 1047–1059. [[CrossRef](#)]
6. Luo, H.; Quaas, J.; Han, Y. Examining cloud vertical structure and radiative effects from satellite retrievals and evaluation of CMIP6 scenarios. *Atmos. Chem. Phys.* **2023**, *23*, 8169–8186. [[CrossRef](#)]
7. Wang, S.; Yi, B. Bibliometric Analysis of Aerosol-Radiation Research from 1999 to 2023. *Atmosphere* **2024**, *15*, 1189. [[CrossRef](#)]
8. Wang, L.; Lu, Y.; Wang, Z.; Li, H.; Zhang, M. Hourly solar radiation estimation and uncertainty quantification using hybrid models. *Renew. Sustain. Energy Rev.* **2024**, *202*, 114724. [[CrossRef](#)]
9. Chen, J.L.; Li, G.S. Estimation of monthly average daily solar radiation from measured meteorological data in Yangtze River Basin in China. *Int. J. Climatol.* **2013**, *33*, 487–498. [[CrossRef](#)]
10. Fan, J.; Chen, B.; Wu, L.; Zhang, F.; Lu, X.; Xiang, Y. Evaluation and development of temperature-based empirical models for estimating daily global solar radiation in humid regions. *Energy* **2018**, *144*, 903–914. [[CrossRef](#)]
11. Prieto, J.-I.; García, D. Global solar radiation models: A critical review from the point of view of homogeneity and case study. *Renew. Sustain. Energy Rev.* **2022**, *155*, 111856. [[CrossRef](#)]
12. Hassan, G.E.; Youssef, M.E.; Mohamed, Z.E.; Ali, M.A.; Hanafy, A.A. New Temperature-based Models for Predicting Global Radiation. *Appl. Energy* **2016**, *179*, 437–450. [[CrossRef](#)]
13. Zhang, J.; Zhao, L.; Deng, S.; Xu, W.; Zhang, Y. A critical review of the models used to estimate solar radiation. *Renewable and Sustain. Energy Rev.* **2017**, *70*, 314–329. [[CrossRef](#)]
14. Yildirim, H.B.; Teke, A.; Antonanzas-Torres, F. Evaluation of classical parametric models for estimating solar radiation in the Eastern Mediterranean region of Turkey. *Renew. Sustain. Energy Rev.* **2018**, *82*, 2053–2065. [[CrossRef](#)]
15. Souza, A.P.; Silva, A.C.; Tanaka, A.A.; Uliana, E.M.; Almeida, F.T.; Klar, A.E.; Gomes, A.W.A. Global radiation by simplified models for state of Mato Grosso, Brazil. *Pesqui. Agropecuária Bras.* **2017**, *52*, 215–227. [[CrossRef](#)]
16. Bender, F.D.; Sentelhas, P.C. Solar Radiation Models and Gridded Database to Fill Gaps in Weather Series and to Project Climate Change in Brazil. *Adv. Meteorol.* **2018**, *2018*, 1–15. [[CrossRef](#)]
17. Martim, C.C.; Souza, A.P. Estimativas da radiação global com base na insolação na Amazônia brasileira. *Rev. Ibero-Am. De Ciências Ambient.* **2021**, *12*, 233–246. [[CrossRef](#)]
18. Delgado, R.C.; Santana, R.O.; Gelsleichter, Y.A.; Pereira, M.G. Degradation of South American biomes: What to expect for the future? *Environ. Impact Assess. Rev.* **2022**, *96*, 106815. [[CrossRef](#)]

19. Silva Junior, C.; Lima, M.; Teodoro, P.E.; Oliveira-Júnior, J.F.; Rossi, F.S.; Funatsu, B.M.; Butturi, W.; Lourençoni, T.; Kraeski, A.; Pelissari, T.D.; et al. Fires Drive Long-Term Environmental Degradation in the Amazon Basin. *Remote Sens.* **2022**, *14*, 338. [[CrossRef](#)]
20. Arévalo, S.M.M.; Delgado, R.C.; Lindemann, D.S.; Gelsleichter, Y.A.; Pereira, M.G.; Rodrigues, R.A.; Justino, F.B.; Wanderley, H.S.; Zonta, E.; Santana, R.O.; et al. Past and Future Responses of Soil Water to Climate Change in Tropical and Subtropical Rainforest Systems in South America. *Atmosphere* **2023**, *14*, 755. [[CrossRef](#)]
21. Jahani, B.; Dinpashoh, Y.; Nafchi, A.R. Evaluation and development of empirical models for estimating daily solar radiation. *Renew. Sustain. Energy Rev.* **2017**, *73*, 878–891. [[CrossRef](#)]
22. Chen, R.; Ersi, K.; Yang, J.; Lu, S.; Zhao, W. Validation of five global radiation models with measured daily data in China. *Energy Convers. Manag.* **2004**, *45*, 1759–1769. [[CrossRef](#)]
23. Abraha, M.G.; Savage, M.J. Comparison of estimates of daily solar radiation from air temperature range for application in crop simulations. *Agric. For. Meteorol.* **2008**, *148*, 401–416. [[CrossRef](#)]
24. Angstrom, A. Solar and terrestrial radiation. *Q. J. R. Meteorol. Soc.* **1924**, *50*, 121–125. [[CrossRef](#)]
25. Prescott, J. Evaporation from a Water Surface in Relation to Solar Radiation. *Trans. R. Soc. South Aust.* **1940**, *46*, 114–118.
26. Hargreaves, G.H.; Samani, Z.A. Estimating potential evapotranspiration. *J. Irrig. Drain. Eng.* **1982**, *108*, 225–230. [[CrossRef](#)]
27. Bristow, K.L.; Campbell, G.S. On the relationship between incoming solar radiation and daily maximum and minimum temperature. *Agricultural For. Meteorol.* **1984**, *31*, 159–166. [[CrossRef](#)]
28. Adaramola, M.S. Estimating global solar radiation using common meteorological data in Akure, Nigeria. *Renew. Energy* **2012**, *47*, 38–44. [[CrossRef](#)]
29. Falayi, E.O.; Adepitan, J.O.; Rabi, A.B. Empirical models for the correlation of global solar radiation with meteorological data for Iseyin, Nigeria. *Int. J. Phys. Sci.* **2008**, *3*, 210–216. [[CrossRef](#)]
30. Santos, C.M.; Teremoto, E.T.; Souza, A.; Aristone, F.; Ilhaddadene, R. Several models to estimate daily global solar irradiation: Adjustment and evaluation. *Arab. J. Geosci.* **2021**, *14*, 286. [[CrossRef](#)]
31. Souza, A.P.; Zamadei, T.; Monteiro, E.B.; Casavecchia, B.H. Atmospheric Transmissivity of Global Radiation in the Amazon Region of Mato Grosso. *Rev. Bras. De Meteorol.* **2016**, *31*, 639–648. [[CrossRef](#)]
32. Li, M.-F.; Tang, X.-P.; Wu, W.; Liu, H.-B. General models for estimating daily global solar radiation for different solar radiation zones in mainland China. *Energy Convers. Manag.* **2013**, *70*, 139–148. [[CrossRef](#)]
33. Newland, F.J. A study of solar radiation models for the coastal region of south China. *Sol. Energy* **1989**, *43*, 227–235. [[CrossRef](#)]
34. Almorox, J.; Hontoria, C. Global solar radiation estimation using sunshine duration in Spain. *Energy Convers. Manag.* **2004**, *45*, 1529–1535. [[CrossRef](#)]
35. Bakirci, K. Correlations for estimation of daily global solar radiation with hours of bright sunshine in Turkey. *Energy* **2009**, *34*, 485–501. [[CrossRef](#)]
36. Ögelman, H.; Ecevit, A.; Tasdemiroglu, E. A new method for estimating solar radiation from bright sunshine data. *Sol. Energy* **1984**, *33*, 619–625. [[CrossRef](#)]
37. Togrul, I.T.; Onat, E. A study for estimating solar radiation in Elazig using geographical and meteorological data. *Energy Convers. Manag.* **1999**, *40*, 1577–1584. [[CrossRef](#)]
38. Togrul, I.T.; Togrul, H.; Evin, D. Estimation of global solar radiation under clear sky radiation in Turkey. *Renew. Energy* **2000**, *21*, 271–287. [[CrossRef](#)]
39. Elagib, N.A.; Mansell, M.G. New approaches for estimating global solar radiation across Sudan. *Energy Convers. Manag.* **2000**, *41*, 419–434. [[CrossRef](#)]
40. El-Metwally, M. Sunshine and global solar radiation estimation at different sites in Egypt. *J. Atmos. Sol.-Terr. Phys.* **2005**, *67*, 1331–1342. [[CrossRef](#)]
41. El-Sebaai, A.A.; Al-Ghamdi, A.A.; Al-Hazmi, F.S.; Faidah, A.S. Estimation of global solar radiation on horizontal surfaces in Jeddah, Saudi Arabia. *Energy Policy* **2009**, *37*, 3645–3649. [[CrossRef](#)]
42. Lee, K.H. Improving the correlation between incoming solar radiation and Sunshine hour using DTR. *Int. J. Climatol.* **2015**, *35*, 361–374. [[CrossRef](#)]
43. Li, M.-F.; Fan, L.; Liu, H.-B.; Guo, P.-T.; Wu, W. A general model for estimation of daily global solar radiation using air temperatures and site geographic parameters in Southwest China. *J. Atmos. Sol.-Terr. Phys.* **2013**, *92*, 145–150. [[CrossRef](#)]
44. Li, H.; Cao, F.; Wang, X.; Ma, W. A temperature-Based model for estimating monthly average daily global solar radiation in China. *Sci. World J.* **2014**, *1*, 128754. [[CrossRef](#)]
45. Li, H.; Cao, F.; Bu, X.; Zhao, L. Models for calculating daily global solar radiation from air temperature in humid regions—A case study. *Environ. Prog. Sustain. Energy* **2015**, *34*, 595–599. [[CrossRef](#)]
46. Goodin, D.G.; Hutchimson, J.M.S.; Vanderlip, R.L.; Knapp, M.C. Estimating solar irradiance for crop modeling using daily air temperature data. *Agron. J.* **1999**, *91*, 845–851. [[CrossRef](#)]
47. Thornton, P.E.; Running, S.W. An improved algorithm for estimating incident daily solar radiation from measurements of temperature, humidity, and precipitation. *Agric. For. Meteorol.* **1999**, *93*, 211–228. [[CrossRef](#)]
48. Weiss, A.; Hays, C.J.; Hu, Q.; Easterling, W.E. Incorporating bias error in calculating solar irradiance: Implications for crop yield simulations. *Agron. J.* **2001**, *93*, 1321–1326. [[CrossRef](#)]

49. Kolebaje, O.T.; Ikusika, A.; Akinyemi, P. Estimating solar radiation in Ikeja and Port Harcourt via correlation with relative humidity and temperature. *Int. J. Energy Prod. Manag.* **2016**, *1*, 253–262. [[CrossRef](#)]
50. Benghanem, M.; Mellit, A. A simplified calibrated model for estimating daily global solar radiation in Madinah, Saudi Arabia. *Theor. Applied Climatol.* **2014**, *115*, 197–205. [[CrossRef](#)]
51. Hargreaves, G.L.; Asce, A.M.; Hargreaves, G.H.; Asce, F.; Riley, J.P. Irrigation water requirements for Senegal river basin. *J. Irrig. Drain. Eng.* **1985**, *111*, 265–275. [[CrossRef](#)]
52. Saffaripour, M.H.; Mehrabian, M.A.; Bazargan, H. Predicting solar radiation fluxes for solar energy system applications. *Int. J. Environ. Sci. Technol.* **2013**, *10*, 761–768. [[CrossRef](#)]
53. Panday, C.K.; Katiyar, A.K. Temperature base correlation for the estimation of global solar radiation on horizontal surface. *Int. J. Energy Environ.* **2010**, *1*, 737–744.
54. Elagib, N.A.; Babiker, S.F.; Alvi, S.H. New empirical models for global solar radiation over Bahrain. *Energy Convers. Manag.* **1998**, *39*, 827–835. [[CrossRef](#)]
55. Ertekin, C.; Yaldiz, O. Estimation of monthly average daily global radiation on horizontal surface for Antalya (Turkey). *Renew. Energy* **1999**, *17*, 95–102. [[CrossRef](#)]
56. Al-Salaymeh, A. Modeling of global daily solar radiation on horizontal surfaces for Amman city. *Emir. J. Eng. Res.* **2006**, *11*, 49–56.
57. Ododo, J.C.; Sulaiman, A.T.; Aidan, J.; Yuguda, M.M.; Ogbu, F.A. The importance of maximum air temperature in the parameterization of solar radiation in Nigeria. *Renew. Energy* **1995**, *6*, 751–763. [[CrossRef](#)]
58. Swartman, R.K.; Ogunlade, O. Solar radiation estimates from common parameters. *Sol. Energy* **1967**, *11*, 170–172. [[CrossRef](#)]
59. Ramos, J.P.A.; Vianna, M.S.; Marin, F.R. Estimation of global solar radiation based on thermal amplitude for Brazil. *Agrometeorol* **2018**, *26*, 37–51. [[CrossRef](#)]
60. Ismail, A.H.; Dawi, E.A.; Almokdad, N.; Abdelkader, A.; Salem, O. Estimation and comparison of the clearness index using mathematical models—Case study in the United Arab Emirates. *J. Nov. Carbon Resour. Green Asia Strategy* **2023**, *10*, 863–869. [[CrossRef](#)]
61. Yang, L.; Gao, X.; Li, Z.; Jia, D. Quantitative effects of air pollution on regional daily global and diffuse solar radiation under clear sky conditions. *Energy Rep.* **2022**, *8*, 1935–1948. [[CrossRef](#)]
62. Yang, L.; Gao, X.; Li, Z.; Jia, D. Intra-day solar irradiation forecast using machine learning with satellite data. *Sustain. Energy Grids Netw.* **2023**, *36*, 101212. [[CrossRef](#)]
63. IBGE_Instituto Brasileiro de Geografia e Estatística. Continuous Cartographic Base—Brazil. 2023. Available online: https://www.ibge.gov.br/geociencias/downloads-geociencias.html?caminho=cartas_e_mapas/bases_cartograficas_continuas/bc250/versao2023/ (accessed on 23 September 2024).
64. Google. Google Earth. Available online: <https://earth.google.com/web> (accessed on 23 September 2024).
65. Alvares, C.A.; Stape, J.L.; Sentelhas, P.C.; Gonçalves, J.L.M.; Sparovek, G. Köppen’s climate classification map for Brazil. *Meteorol. Z.* **2013**, *22*, 711–728. [[CrossRef](#)] [[PubMed](#)]
66. WMO_Word Meteorological Organization. Guide to Meteorological Instruments and Methods of Observation. 2014. Available online: https://community.wmo.int/en/activity-areas/imop/wmo-no_8 (accessed on 1 October 2024).
67. Allen, R.G.; Pereira, L.S.; Raes, D.; Smith, M. *Crop Evapotranspiration Guidelines for Computing Crop Water Requirements—FAO Irrigation and Drainage Paper 56*; Food and Agriculture Organization of the United Nations: Rome, Italy, 1998; 333p.
68. Bahel, V.; Bakhsh, H.; Srinivasan, R. A correlation for estimation of global solar radiation. *Energy* **1987**, *12*, 131–135. [[CrossRef](#)]
69. Glover, J.; McCulloch, J.S.G. The empirical relation between solar radiation and hours of sunshine. *Q. J. R. Meteorol. Soc.* **1958**, *84*, 172–175. [[CrossRef](#)]
70. Korachagaon, I.; Bapat, V.N. General formula for the estimation of global solar radiation on earth’s surface around the globe. *Renew. Energy* **2012**, *41*, 394–400. [[CrossRef](#)]
71. Badescu, V. Assessing the performance of solar radiation computing models and model selection procedures. *J. Atmos. Sol. -Terr. Phys.* **2013**, *105*, 119–134. [[CrossRef](#)]
72. Teke, A.; Yildirim, H.B.; Çelik, Ö. Evaluation and performance comparison of different models for the estimation of solar radiation. *Renew. Sustain. Energy Rev.* **2015**, *50*, 1097–1107. [[CrossRef](#)]
73. Escobedo, J.F.; Gomes, E.N.; Oliveira, A.P.; Soares, J. Modeling hourly and daily fractions of UV, PAR and NIR to global solar radiation under various sky conditions at Botucatu, Brazil. *Appl. Energy* **2009**, *86*, 299–309. [[CrossRef](#)]
74. Araújo, W.F.; Neto, J.L.L.M.; Sander, C.; Albuquerque, J.A.A.; Viana, T.V.A.; Valero, M.A.M. Update on the climate classification of Boa Vista, Roraima, Brazil. *Nativa* **2024**, *12*, 236–240. [[CrossRef](#)]
75. Sabino, M.; Silva, A.C.; Almeida, F.T.; Souza, A.P. Reference evapotranspiration in climate change scenarios in Mato Grosso, Brazil. *Hydrology* **2024**, *11*, 91. [[CrossRef](#)]

Disclaimer/Publisher’s Note: The statements, opinions and data contained in all publications are solely those of the individual author(s) and contributor(s) and not of MDPI and/or the editor(s). MDPI and/or the editor(s) disclaim responsibility for any injury to people or property resulting from any ideas, methods, instructions or products referred to in the content.